POLITECNICO DI TORINO

Corso di Laurea Magistrale

in Ingegneria Energetica e Nucleare

Tesi di Laurea Magistrale

Closed-loop systems for geothermal resources exploitation from hydrocarbon wells

Relatore:

Stefano Lo Russo

Correlatore:

Glenda Taddia

Martina Gizzi

Candidato:

Alessandro Bologna

Anno Accademico 2019/2020

Abstract

Below the surface of the earth, there exist geothermal resources with the potential to make a significant contribution to the increasing demand of power consumption and environmental sustainability. However, the expensive capital costs of drilling the geothermal well still represent the main challenge to the implementation of this resource in energy systems.
Dismissed hydrocarbon wells in mature oilfields can be considered good candidates for the geothermal energy exploitation as they usually have high bottom-hole temperature, reliable wellbore integrity and large production capacity.
Existing borehole and perforation data can be also useful to have geological, geophysical and geochemical information about the sub-surface reservoirs and allow direct access to the sub-soil heat.

In different studies of the past years, authors were oriented in the direction of the implementation of open loop systems by using directly oil or gas reservoir as a geothermal reservoir.
Another way to recover heat is to convert the considered borehole into a heat exchanger using closed-loop system: this kind of system allows to extract heat from the ground without requiring any water to be abstracted or re-injected at all.
In the developed thesis work, the attention was centred on two different closed-loop-type technologies: U-tube and coaxial Wellbore Heat Exchanger (WBHE). The selected case study is located in one of the largest European oil fields: Villafortuna Trecate oilfield, active since 1984. The extracted heat it has been hypothesized to be used either for district heating or other direct uses.
Two different heat exchange models (U-tube and coaxial WBHE) have been implemented in MATLAB software with the main aims to 1) find the best configuration that allows to maximize the heat recovery from the soil, examining the main factors affecting the extraction efficiency; 2) understand the technical feasibility of such retrofitting project from a hydrocarbon well to a geothermal one.

The results have shown that thermal power extracted from this type of applications depends mainly on geological parameters, such as site stratigraphy, and on technical parameters related to the plant, such as depth, diameter of the well and insulating material.

Index

List of Tables

List of Figures

1. Introduction

During the last century, energy production strategy exclusively based on fossil fuels has caused an enormous impact on humanity and the environment, from air and water pollution to global warming. The limits of this type of energy system in terms of air pollutant emissions and resource depletion have taken on more and more evidence over the last few decades.
In this context, clean energy production by means of renewable resources has become one of the major challenges the world faces today and one of the central topics of the European development policies: medium-long term objectives concerning the decarbonisation of the European Energy Systems is corroborated in the 2020 Climate and Energy Package and the following 2030 climate and energy framework.
More progress needs to be made regarding the integration of renewable energy in end-use applications in buildings, transportation and industries in urban areas to transform global energy systems. The primary aim of energy companies has become to provide energy solutions that are increasingly sustainable and distant from those based on fossil fuel, through technological development and environmental protection values.
Geothermal energy as a renewable and sustainable energy source could play a key role in this process. In particular, the production of a new type of clean energy based on the exploitation of available deep geothermal resources that are associated with abandoned oil and gas wells could represent a considerable future potential. Dismissed hydrocarbon wells in mature oilfields represent best candidate structures for the geothermal energy exploitation as they usually have high bottom-hole temperature, reliable wellbore integrity and large production capacity.
Although the oilfield geothermal resource is gaining increasing attention and scientific knowledge has achieved a notable degree of development, there still exist challenges that further limit its use. The majority of works that have been carried out on existing abandoned petroleum wells have focused on open-loop systems designed to reuse petroleum fields as geothermal reservoirs. However, open-loop technologies were found to be subject to some technical problems, including groundwater recession, corrosion and scaling problem. A further issue was represented by the re-injection of fluids.
An effective alternative to open loop-technologies was found in the use of closed-loop deep geothermal systems (wellbore heat exchangers - WBHEs).
With the general aim of deepening the knowledge of the different technologies that allow to take advantage of the thermal resources associated with dismissed oil and gas wells in oilfields, several stages of analysis have been developed in this work.

In the first phases of work the attention was focused on two different closed-loop-type technologies: U-tube and coaxial Wellbore Heat Exchanger (WBHE).
Two different heat exchange models (U-tube and coaxial WBHE) have been implemented in MATLAB software with the main purposes to 1) examine the main factors affecting the extraction efficiency; 2) find the best closed-loop configuration that allows to maximize the heat recovered from the soil.
With the purpose of obtaining information about the energy performances associated with open geothermal systems, open-loop technologies results have also been analyzed.
The second phases of work were dedicated to an evaluation of different coaxial-WBHE configurations, two optimization processes have been carried out with an energy and economic focus.
Given the complexity of the problem to not be trapped in some of the local minima of an objective function, a metaheuristic approach was chosen and a particle swarm optimization was performed.
The selected case study is represented by one of the main abandoned oil and gas fields in Italy: Villafortuna–Trecate Field. The final use of the extracted heat was hypothesized to be intended for direct applications, such as a possible district heating system built in the oilfield nearby area.

2. Geothermal energy resources in italian oil and gas fields

Geothermal energy is represented by the heat derived from the sub-surface of the earth. By means of the term geothermal gradient the geologists express the increase in temperature with depth in the Earth's crust. Down to the depths accessible by drilling with modern technology (about 10.000 m) the average geothermal gradient is about 2.5-3C/100 m. It was demonstrated that a portion of potentially exploitable geothermal energy resources is hosted in sedimentary basins [1].
In particular, geothermal energy resources associated to existing OilGas wells in Italian hydrocarbon basins represent an increasingly a considerable economic resource.
A variety of petroleum systems were identified in Italy, as a result of a complex geological and sedimentary history.
Among the different European countries, Italy has one of richest evidences of hydrocarbon seepages: the populations that have inhabited the country during the various historical periods took advantage of these phenomena, harvesting oil and bitumen from the surface [2].
In different bibliographic works, synthetic overviews of the Italian peninsula and its surrounding marine areas geological evolution were provided [3], [4], [5].
As also described by the mentioned authors, Italian hydrocarbon occurrences can be classified as associated to three main tectono-stratigraphic systems:

- carbonate Mesozoic substratum of the foredeep/foreland area and of the external thrust belts;
- thrusted terrigenous Oligo-Miocene foredeep wedges (Southern Alps, Northern Apennines, Calabria and Sicily;
- terrigenous Pliocene-Pleistocene successions of the late foredeep basins of the Apennines, in both central and northern Adriatic Sea and in the Po Plain.

At least five important source rocks have been recognized, distributed in age from Mesozoic through Pleistocene. Three of them were deposited during Mesozoic crustal extension and are mainly oil-prone.
Villafortuna–Trecate (Po Plain), Val d'Agri/Tempa Rossa (southern Apennines) and Gela (Sicily)

fields represent the largest oil accumulations pertaining to these systems.
Considering the large number of existing oil and gas wells that are abandoned and dismissed every year in Italian oilfields and the temperatures-range associated with hydrocarbon fields oil and gas deep wells usually between 65 and 150 C, many authors have started to hypothesize the implementation of new strategies and engineering tools for understanding the possibility of the exploitation of this type of thermal resource.
In this work, the attention is focused on the analysis of the thermal potential associated with disused hydrocarbon wells located within the of Villafortuna-Trecate field.

2.1 Villafortuna–Trecate Field (Po Plain)

Villafortuna–Trecate system represents one of the largest oil accumulations pertaining to the Italian Middle Triassic petroleum system. Because of its depth, it can be pursued only in the outer sector of the foredeeps and in foreland regions (Piedmont area), whereas along the thrust belt it is generally too deep (Po Valley).

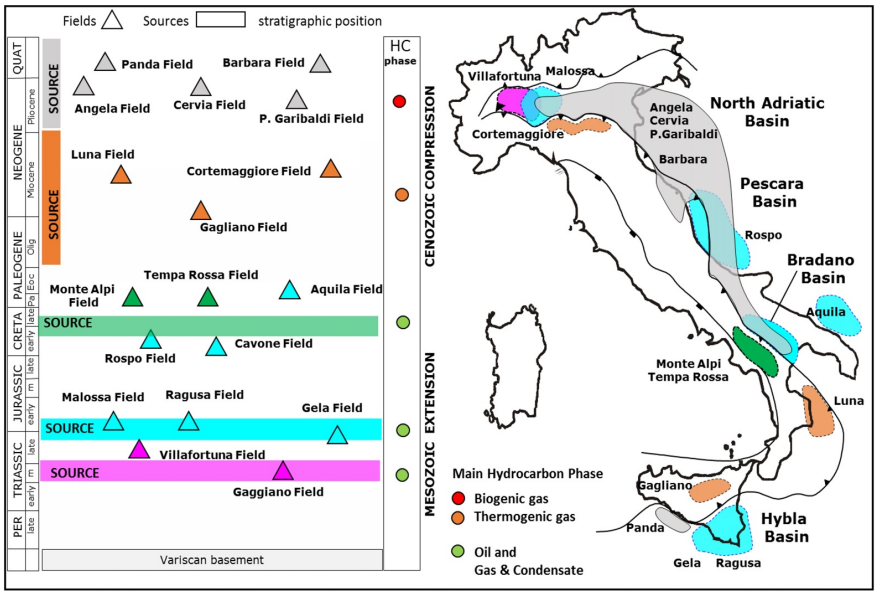

Figure 2.1: Stratigraphic and geographic location of the Italian petroleum systems.. Modified from [5]

The Villafortuna Field, discovered in 1984 in northern Italy, and its Trecate extension constitute the largest oil accumulation pertaining to this petroleum system [5].
The main reservoir associated with the Villafortuna-Trecate Oil field was identified at between 5800 m and 6100 m depth with an available temperature of approximately 160–170 C. The original volume of oil in place (OOIP) was estimated about 300 million barrels [6].
Data related to litho-stratigraphic information and temperature data visualization of the Villafortuna-Trecate area (hydrocarbon wells perforation data) are available by accessing on The Italian National Geothermal Database (BDNG).
The BDNG represents the largest collection of Italian Geothermal data and was set up in the 1980s.

It was implemented by the Institute of Geosciences and Earth Resources (IGG) of the National Research Council (CNR) of Italy.
In particular, for the analysis and the elaborations carried out within this work, it has been used the available bibliographic information of a disused hydrocarbon well of the Villafortuna-Trecate area (Villafortuna 1 well).

Table 2.1: Villafortuna stratigraphy data

Depth	Litho-stratigraphic profile	Age	Thickness	kr	ρscs	ρs
m			m	W/mK	kJ/m3K	kg/m3
609	Depositi fluido-glaciali	/	609	/	/	/
1258	Formazione sabbie di Asti	Pleistocene	649	0.30	800	1700
1405	Argille del santerno	Pliocene inferiore	147	1.61	1696	1890
1660	Formazione gonfolite	Aquitaniano	255	3.16	1937	2359
2611	Formazione gallare	Aquitaniano	951			
4457	Formazione gonfolite	Oligocene	1846			
4560	Formazione gallare	Oligocene inferiore	103			
5430	Formazione scaglia	Cretaceo superiore	870			
5493	Marne del bruntino	Albiano	63			
5568	Maiolica	Cretaceo inferiore	75	3.50	2010	2480
5573	Formazione selcifero	Malm	5			
5586	Formazione medolo	Lias	13			
6132	Calcari di meride	Triassico medio	546			
6202	Dolomia di S. Salvatore	Triassico medio	70			

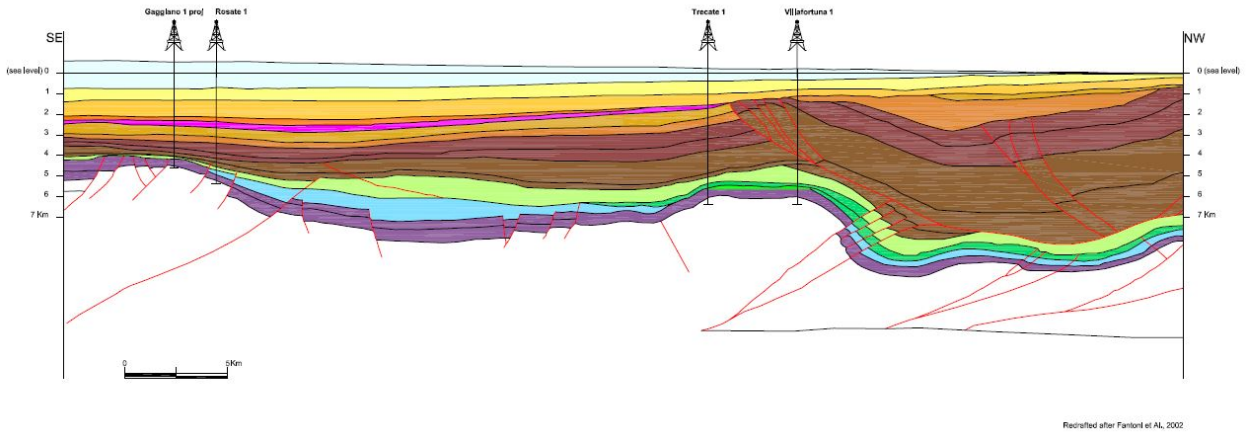

Figure 2.2: Villafortuna graphic representation of stratigraphy

2.2 Heat transfer processes in oil and gas fields

In oil and gas fields, such as the one analysed in this work (Villafortuna - Trecate oilfield), the formation of geothermal resources results from interactions between different processes comprising groundwater flow, mass transport and heat transfer and different water–rock interaction mechanisms. In detail, the heat transfer processes occur through two main processes: conduction and convection [7].

Conduction

Conduction represents the transfer of heat energy by means of the direct contact between substances in which a temperature gradient exists:

$$q_x = -\lambda \cdot \frac{dT}{dX} \tag{2.1}$$

Where q is the amount of heat per unit area exchange in the direction x, $\frac{dT}{dX}$ is the thermal gradient in the direction x and λ is the material conductivity.

Convection

Convection represents the heat exchange between two surfaces by a fluid in motion through molecular interaction. As for conduction, also in this case the transfer of heat occurs only if a temperature gradient exists. The phenomenon is ruled by the following equation:

$$q = h \cdot (T_\infty - T_s) \tag{2.2}$$

Where T_∞ is the temperature of the free stream outside the velocity boundary layer, and Ts is the temperature of the surface on which convection is considered. h is a parameter that depends on the geometry of the system, the thermodynamic properties of the fluid, the thermal properties of the solid medium and the systems boundary conditions. The Nusselt number (Nu) can be used to estimate the value of h following the equation below

$$h = \frac{\lambda \cdot Nu}{D} \tag{2.3}$$

D is the equivalent diameter.

Nu is a number depends on two dimensionless parameters Reynold (Re) and Prandlt (Pr) number.

The Prandlt number (Pr) is the ratio of momentum diffusion rate to thermal diffusion rate; The Reynold number (Re) predicts the flow behaviour of the fluid.

The correlation between Nusselt number, Reynold and Prandtl number strictly depends on the flow conditions.

Nusselt correlation	Author	Flow conditions
$N_u = 0.023 Re^{4/5} Pr^n$	Dittus and Boelter (1930)	$0.7 \leq Pr \leq 160$ $Re \geq 10000$
$N_u = 0.027 Re^{4/5} Pr^{1/3} \left(\frac{\mu}{\mu_s}\right)^{0.14}$	Seider and Tate (1936)	$0.7 \leq Pr \leq 16700$ $Re \geq 10000$
$N_u = \frac{(f/8)(Re-1000)Pr}{1+12.7(f/8)^{1/2}(Pr^{2/3}-1)}$	Gnielinski (1976)	$0.5 < Pr < 2000$ $2300 < Re < 500,000$
$N_u = 4.36$		$Re < 2300$

Figure 2.3: Convection correlations for circular tubes[7]

Understanding the relative impact of different heat transfer processes in oilfields by means of the interpretation of their physical laws is of crucial importance in the planning phase of a new geothermal energy fields exploitation project.

3. Closed-loop systems:Wellbore heat exchangers (WBHEs)

In order to exploit geothermal energy resources associated to decommissioned hydrocarbon wells, it is required that the considered borehole is retrofitted in a heat exchanger.
A possible technology is represented by the use of closed-loop systems: U-tube and coaxial heat exchangers represent two common types of available systems to be implemented in a disused hydrocarbon well. This kind of system allows to extract heat from the ground without requiring any water to be abstracted or re-injected at all. Therefore, it can be constructed practically anywhere.
In the tubes of a closed-loop system both water or other fluids can flow to enhance the heat transfer and improve the efficiency of the system.
The consequences of corrosion are taken into account in the selection phase of the carrier fluid: the selected fluid can be very good for exchanging heat but, at the same time, it can reduce a lot the life of the system. In some cases, the maintenance of this type of system could become very difficult and expensive.
Due to its low cost and capacity to transfer and store heat, one of the most used fluids is the water.
In closed-loop configuration, as there is no direct pumping of the ground water, all the problems connected with the exploitation of the ground (water treatment and disposal) don't occur overall.
The advantages of this type of configuration are represented by lower costs and less operational complications.
In addition, system operating parameters such as the fluid flow rate and pipe diameter have to be selected in order to guarantee the following conditions:

- Achieve transient – turbulent flow conditions in the subsurface closed loop (turbulent conditions facilitate heat transfer from the ground to the fluid);

- Kept acceptably low hydraulic head losses (and thus energy expended on circulation pumping).

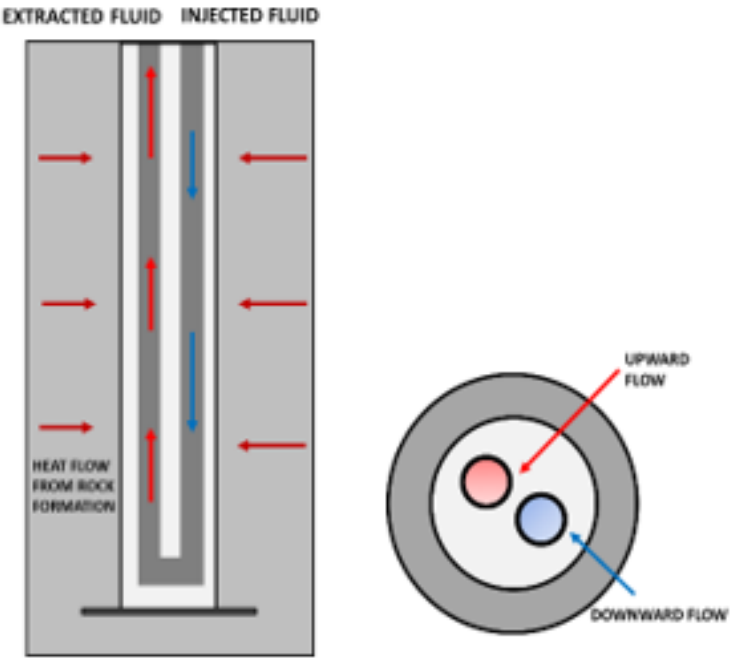

Figure 3.1: Schematic representation of a U-tube

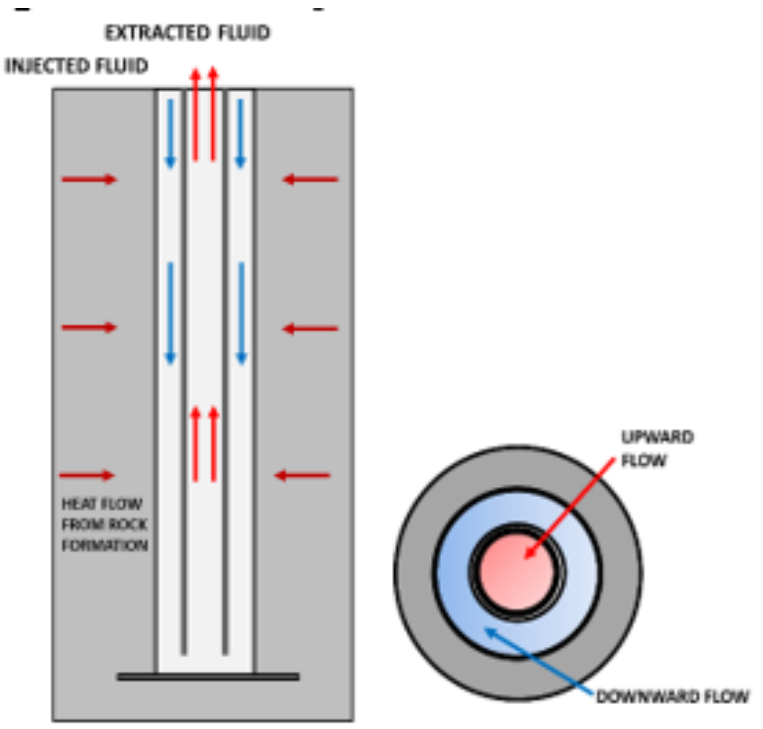

Figure 3.2: Schematic representation of a coaxial heat exchanger

3.1 Coaxial closed-loop system

A double-pipe (coaxial tube) heat exchanger is installed into a wellbore by inserting a single tube of inferior size. The fluid is forced to go down through the annulus and go up in the inner tube: in this configuration the fluid has enough time to gain heat conducted from surrounding rocks and transfer thermal energy back to the surface.
When the fluid reaches the bottom, it goes up in the inner tube up to the wellhead. Between the annulus and the internal tube there is a gap, usually filled with an insulating material to keep high the water temperature.
In this type of configuration, the heat exchange area is also bigger than in U-tube configuration with an improving of the system associated with an increase of the outer temperature of the fluid (considering same flow rate) and of the applicability of this heat to a larger kind of exploitation by the users.
In addition, in this type of system the hole between the external tube and ground is filled with grout, in order to prevent the direct leakage between ground and tubes and to avoid the connection between ground and surface.

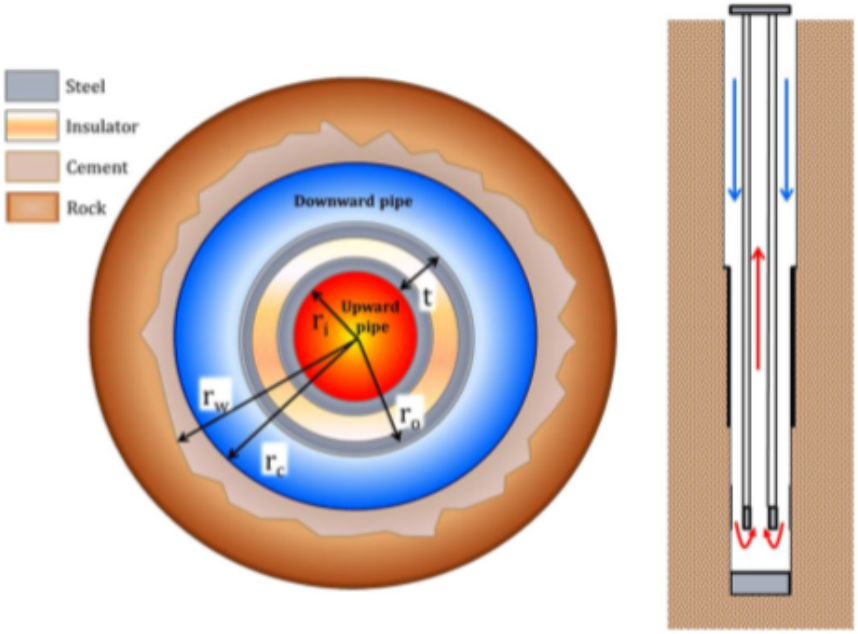

Figure 3.3: Wellbore heat exchange. Cross and schematic sections[8]

In order to evaluate and analyse the temperature profile of the water and to find the best system-configuration the model proposed below was applied.
The aim assumption of the model is:

- heat in the reservoir propagate by means of conduction (the convection in the reservoir rock is neglected); inside the tubes takes place conduction and convection phenomena.

Downward tube

The steel downward tube is cemented to the rock wall, so it is in contact with the well hole. The heat exchange in the ground and in the tube is due by conduction instead between pipe and fluid is convection.
The energy balance equation of the fluid in the outer pipe (injection pipe) of a coaxial WBHE can be expressed as the following equation.

$$\frac{d((\rho \cdot Cp)_f \cdot A_0 \cdot T_{fo})}{dt} + \frac{d((\rho \cdot c)_f \cdot A_0 \cdot v_f \cdot T_{fo})}{dz} = -\frac{dQ}{dz} + \frac{dQ_{i0}}{dz} \tag{3.1}$$

where:

-A_0 and v_f are the outer pipe area and fluid velocity.

-T_{fo} is the fluid temperature in the outer pipe.

-$\frac{dQ}{dz}$ is the heat extraction from formation at unit of well depth [$\frac{W}{m}$].

Although insulation is used to prevent heat loss from the inner pipe fluid, heat is partly transferred between the two pipes: $\frac{dQ_{i0}}{dz}$ represents the heat flux from the inner pipe to the outer pipe. Therefore, the energy equation for the inner pipe can be given as

$$\frac{d((\rho \cdot Cp)_f \cdot A_i \cdot T_{fi})}{dt} + \frac{d((\rho \cdot c)_f \cdot A_i \cdot v_f \cdot T_{fi})}{dz} = -\frac{dQ_{i0}}{dz} \tag{3.2}$$

By assuming steady heat transfer and constant heat flux in wellbore components (insulation, casing, cement), the heat extraction from formation dQ/dz can be assumed equal to the heat flux through the outside surface of the wellbore (interface of wellbore/rock formation) to the injected fluid [9][10]

$$\frac{dQ}{dz} = 2 \cdot \pi \cdot r \cdot k_t \cdot (T_v(\mathbf{z}) - T_{f,down}) \tag{3.3}$$

The total amount of heat power transferred by ground to the fluid can be expressed as[8]:

$$Q = 2 \cdot \pi \cdot r \cdot k_t \cdot (T_v(\mathbf{z}) - T_{f,down}) \cdot \Delta z \tag{3.4}$$

where:

- r external radius of the borehole.

-kt total heat exchange coefficient.

-Tv rock temperature at depth z.

-Tf,down water temperature in external tube.

-Δz length of the pipe.

kt, the total heat exchanger coefficient, is represented by the sum of the heat transfer components, expressed as thermal resistances as

$$R_t = R_a + R_c + R_s \tag{3.5}$$

where

- Ra represents the heat transfer by convection into the pipe.

- Rc represents heat transfer by conduction through the casings of the well component.

- Rs represents thermal resistance due to the heat transfer by conduction in the rock and function of time .

The thermal ground resistance (R_s) depends on time; the radius of influence (r_s) that take in account this phenomenon, can be determined using the following relationship

$$r_s = 2 \cdot \sqrt{\alpha_s \cdot t} \tag{3.6}$$

where:

- t is the elapsed time since start.

- α_s is the rock thermal diffusivity.

$$\alpha_s = \frac{\lambda}{(\rho \cdot Cp)} \tag{3.7}$$

This parameter increases very rapidly in time, mainly in the first period. Consequently, also the thermal resistance Rs increases in time.

$$R_s = \frac{1}{(2 \cdot \lambda)} \cdot \ln \frac{r_s}{r_w} \tag{3.8}$$

where:

- λ is the thermal conductivity of the rock.

- r_w is the external radius of the well.

Ra represents the component correlated with the convective part inner the tube: it is evaluated by means of the Nusselt number as in the following equation

$$h = \frac{Nu \cdot \lambda_f}{D_h} \tag{3.9}$$

where:

-D_h is the hydraulic diameter.

-h is the convective heat transfer coefficient.

The Nusselt number can be evaluated, assuming turbulent flow inside the tube, as

$$Nu = 0.023 \cdot Re^{0.8} \cdot Pr^{0.4} \tag{3.10}$$

where:

$$Pr = \frac{Cp \cdot \mu}{\lambda} \tag{3.11}$$

$$Re = \frac{\rho \cdot v \cdot D}{\mu} \tag{3.12}$$

Rc, the tube resistance, is determined as:

$$Rc = 0.5 \cdot \sum_{i=1}^{n} \frac{1}{\lambda_i} \cdot \frac{r_{c,i+1}}{r_{c,i}} \tag{3.13}$$

Rc can be neglected in the total resistance calculation, due to the high thermal conductivity of the steel piping.

The total heat exchanger coefficient can be determined as in the following Equation

$$\frac{1}{k_t} = \frac{D_c}{(2 \cdot \lambda)} \cdot \ln \frac{r_s}{r_w} + \frac{1}{h} \tag{3.14}$$

where:

- $D_c = D_w$, the thickness of the tube is negligible.

Upward tube

At the well bottom, the heated fluid is forced to enter and flow through the internal pipe of the coaxial WBHE. Going up to the wellhead, heat transfer occurs only through the wall of the internal pipe. Thus, $\frac{dQ_{i0}}{dz}$ is determined by considering the temperature difference between the outer pipe and inner pipe fluids, together with the estimated thermal resistance insulation value.

$$\frac{dQ_{i0}}{dz} = 2 \cdot \pi \cdot r_0 \cdot k_0 \cdot (T_{f,up} - T_{f,down}) \tag{3.15}$$

The total heat exchange in upward tube is described by the Equation:

$$Q_{i0} = 2 \cdot \pi \cdot r_0 \cdot k_0 \cdot (T_{f,up} - T_{f,down}) \cdot \Delta z \tag{3.16}$$

where:

- r_0 is the internal radius of the pipe.

- k_0 is the heat transfer coefficient referred to the internal radius.

K0 is composed by three components: the two convective components and one conductive due to the tube.

$$\frac{1}{k_0} = \frac{r_0}{r_0 + d} \cdot \frac{1}{h_i} + r_0 \cdot \ln \frac{r_{i+1}}{r_i} \cdot \frac{1}{\lambda_i} + \frac{1}{h_0} \tag{3.17}$$

where:

- d is the thickness of the tube.

- h_i is the inner tube convective coefficient.

- h_0 is the outer tube convective coefficient.

- λ_i is the thermal conductivity of the material.

Pressure losses

The heat-exchange is not the only aspect to take in account, also the pressure losses must be considered as they affect pumping cost, not negligible in the management of the system.

$$\Delta P = \rho \cdot g \cdot \Delta z - \Delta P_f Downward \tag{3.18}$$

$$\Delta P = -\rho \cdot g \cdot \Delta z - \Delta P_f Upward \tag{3.19}$$

The first term strictly depends by the elevation.
The second is due by the friction and it depends on velocity:

$$\Delta P_f = \frac{f \cdot \Delta z}{D} \cdot \rho \cdot \frac{v^2}{2} \tag{3.20}$$

Where:

- f is the friction factor.

- Δ z is the length of the pipe.

- D is the diameter of the circuit. For the inner tube, D is the diameter of the tube while for the annulus D is the hydraulic diameter evaluated as $D_h = \frac{4 \cdot area}{wetperimeter}$.

- v is the fluid velocity.

The loss of pressure due to the elevation is zero, adding the upward and downward components.
The components due the friction is different from zero and the pump must give the power to equilibrate this component. The upward and downward ΔP is not equal because the velocity and diameter change in the two configurations.

3.2 Models for the profile temperature evaluation

The works carried out by Kujawa et al. [11][12] represent the pioneering researches for the evaluation of the possibility to retrofit abandoned oil and gas wells for geothermal energy exploitation, utilising a coaxial WBHE.
In their studies, they proposed a 2870-m-long coaxial WBHE for a Jachowka K-2 well with an external casing constituted by a column of steel pipes with diameters of 244.5/222.0 mm and a new column of pipes with diameters of 60.3/50.7 mm, located concentrically inside the exchanger. Due to their starting assumptions of a steady state and a constant temperature at the interface of wellbore/formation, they considered a simplified heat exchange model in which the heat flux penetrating from the external fluid is equal to the heat flux conducted through the multilayer cylindrical barrier and to the heat flux penetrating the internal fluid.
In detail, they started from the formula of linear density of the heat flux transferring from one medium and estimated the overall heat transfer coefficient between the outer pipe fluid and wellbore outside (kw) by using equations provided by Charnyi [13][14] and Dyad'kin and Gendler [15]

$$k_w = \frac{k_w^{'}}{(1 + Bi \ln(1 + \sqrt{\gamma \cdot F0})} \tag{3.21}$$

$$\frac{1}{k'_w} = \frac{1}{h_f} + \frac{D_1}{2} \cdot \sum_{i=1}^{n} \frac{1}{\lambda_i} \cdot \frac{D_{i+1}}{D_i} \tag{3.22}$$

where Bi=$\frac{h_f \cdot r_c}{\lambda_s}$ is the Biot number, Fo=$\frac{a_s \cdot t}{r_c^2}$is the Fourier number and is the parameter depending on the Biot number (if Bi>30,$\gamma = \pi$. In other cases, $\gamma = 2$).

By performing calculations for selected volume flow rates of injection fluid (water) flowing through the heat exchanger (2, 10, 20 and 30 $\frac{m^3}{h}$) and temperatures respectively equal to 10, 15, 20, and 25C, the authors demonstrated the practical significance of reusing the existing well for only two injection flow rate values: 2 and 10 $\frac{m^3}{h}$, with associated temperatures at the extracted fluid of 65C and 47C, respectively.

Furthermore, Bu et al.[16][17] began to consider heat transfer from geological formations as being associated to two-dimensional heat conduction phenomena by replacing the assumption of constant temperature at the interface of wellbore/formation in Kujawa et al. [11][12] and Davis and Michaelides [18].

Through analysing abandoned wells that were 4000 m deep with an associated geothermal gradient of 25 C/km and 45C/km, Bu et al. [16][17] discretised energy balance equations for coaxial WBHE using the finite volume method and solving it using the tri-diagonal matrix algorithm (TDMA) [19].

Although they considered the heat transfers from geological formations as transient in their study, a finite boundary was set for surrounding rocks with the assumption that rock temperature became constant at a radius of surrounding rocks over 200 m.

For their elaborations, the diameter of the injection well on the top part was fixed to 340/300 mm with a length of 2500 m, while the bottom diameter was 330/300 mm with a length of 1500 m. The inner diameter of the extraction well was 100 mm.

For a selected geothermal gradient of 45 C/km, they estimated net power output for the analysed single well of 53.70 kWe with an outlet temperature is 129.88 C. The optimal flow velocity of the fluid at which they attained the maximum net power was 0.03 [m/s], while the maximum value of heat from rocks was acquired at a flow rate of 0.05 [m/s].

Different from Bu et al.[16][17], Cheng et al. [20][21] examined the effects of formation heat transfer with an infinite boundary and conducted a theoretical analysis of geothermal power generation from abandoned wells using isobutane as the working fluid. In their study, they started from Ramey's (1962)[22] definition of radial heat flow from the formation at the heat exchanger/formation interface and introduced a novel transient heat conduction function f(t), as follows.

$$\frac{dQ}{dz} = \frac{(2\pi\lambda_s(T - T_w))}{f(t)} \tag{3.23}$$

where T is the formation temperature at an infinite distance from the well axis, T_w is the heat exchanger/formation interface temperature and λ_s is the thermal conductivity of the rock formation.

Different from the traditional f(t) introduced by Ramey (1962)[22] that only considered the effect of time, the novel transient heat conduction function obtained by Cheng et al.[20][21] allowed the consideration of the effect of time and heat capacity of the wellbore on heat extraction from formation.

$$f(t) = \frac{(16\omega^2)}{\pi^2} \int_0^\infty \frac{(1 - \exp(-t_D u^2)}{(u^3 \Delta(u, \omega))} \tag{3.24}$$

where $t_D = \frac{\alpha_s t}{r_i^2}$ is defined as dimensionless time, r_i is the inner radius of the injection well, α_s is the thermal diffusivity of the formation, ω is the ratio of the formation heat capacity and the wellbore heat capacity, u is the variable for integration and the function $\Delta(u, \omega)$ is associated to the following relation.

$$\Delta(u, \omega) = (uY_0(u) - \omega Y_1(u))^2 + (uJ_0(u) - \omega J_1(u))^2 \tag{3.25}$$

where J_0 and J_1 are the zero-order Bessel function of the first kind and the first-order Bessel function of the first kind, respectively. Y_0 and Y_1 are the zero-order Bessel function of the second kind and the first-order Bessel function of the second kind, respectively.

The results of their studies, which were performed on an abandoned well with a depth of 6000 m, clearly showed for the first time how geothermal power generation is strongly influenced by the formation of heat transfer mechanisms.

Furthermore, they determined that the outlet temperature of working fluid tends to gradually decrease with increasing operating time, eventually approaching a steady state. The inlet velocity of isobutene in the injection well was also a binding parameter, as the heat obtained from abandoned well and fluid outlet temperature strongly decreased with increasing fluid inlet velocity.

Meanwhile, Templeton et al.[23] also developed a two-dimensional cylindrical model by incorporating Fourier's three-dimensional diffusion law, two different terms describing the unsteady state heat transfer in the heat exchanger, the advective and conductive effects of the working fluid into the energy conservation equation, to generate a partial differential equation that properly describes the heat transfer mechanisms.

Comparing the results obtained from the proposed model with the ones reported in Kujawa et al.[12] and Bu et al. [16], they clearly showed that the use of a one-dimensional model tends to overestimate the performance of a coaxial WBHE.

More recently, Alimonti and Soldo[8] also focused on the optimisation of a coaxial WBHE structure to maximise the heat extraction from an abandoned oil and gas well located in one of the largest European oil fields, the Villafortuna Trecate Oilfield. The main reservoir associated with this site was identified at between 5800 m and 6100 m depth with an available temperature of approximately 160–170 C.

The same approach described by Kujawa et al. [11][12] was proposed and implemented in a C-computation code for simulating formation heat conduction mechanisms.

The ground resistance, depending on time, used is the eq. 3.8, the resistance is computed with the aims of another parameter called radius of influence eq. 3.6, that take into account the time influence.
By fixing the sizing of the inner and outer tubes, as well as the final casing size as reported in Table 3.1 with an inlet temperature of the heat carrier fluid equal to 40 C, they analysed variations in the temperature of the extracted fluid as a function of different fluid flow rate values.
The results, performed by considering the properties of rocks to be uniform with depth (λ_s 2.5 $\frac{W}{mK}$, ρ 2600 $\frac{kg}{m^3}$ and Cp_s 800 $\frac{J}{m^3 \cdot K}$) demonstrate how the fluid temperature reaches a maximum value of approximately 120 C for an injection fluid flowrate of 10 $\frac{m^3}{h}$. Also, the increase in injection flowrate values tended to always cause a decrease in the recorded temperatures at the wellhead.

Table 3.1: WBHE tube sizing– ID: internal diameter, OD: external diameter.[8]

Tube sizing	ID (mm)	OD (mm)
3 inches	77.9	88.9
5 inches	121.4	139.7
Casing 7 inches	150.4	177.8

3.3 Model assumptions and description

Matlab is a software for the numerical and statistical calculations, written in C language.
As Matlab software allows to easily solve algorithms, it is used to perform this type of analysis on both coaxial and u-tube geothermal system.

Assumptions and approximations:

- The profile temperature in the radial direction is assumed to be constant. Therefore, there is no temperature gradient in the annulus and in the inner tube: due to the turbulent flow, a very enhanced mixing phenomena occur, decreasing the radial gradient.
The temperature changes only in the annulus and inner tube vertical direction, so that the profile of the temperature is unidirectional (vertical only).

- The properties of the heat carrier fluid are assumed constant. As in the case considered the fluid is water (connoted by subscript w), no variations will occur due pressure or/and temperature gradient.

- The model is performed in steady state condition, no temperature variation occur during time, each point in the tubes (annulus and inner tube) keep the same temperature for the entire life. Consequently, the model doesn't take in account the transitory processes.

- The model considers negligible the resistance associated to the thickness of the tubes. The tubes material has a very high conductivity so that its resistance can be considered small compared to the other resistances in the system. - For the resistance associated to the rock 3.6, the time value used is 3 years after the starting of the system. This assumption makes this method conservative. (The system in the years before work better- the temperature and the heat exchange are bigger).

- For the calculation of the annulus dimensionless numbers is used the hydraulic diameter [24]

$$D_h = \frac{4 \cdot area}{wetperimeter} \tag{3.26}$$

The fluid is forced to go down through the annulus and go up through the inner tube. The model follows the path of the fluid with an approach step by step. In detail, the model considers intervals of length dz; in each interval dz, inlet and outlet temperature are calculated, by solving the energy balance equation for each volume dv. For the estimation of the energy exchange in the radial direction is used the mean value of the temperature in the volume dv, calculated through the arithmetic mean

$$T_m = \frac{(T_{inlet} + T_{outlet})}{2} \tag{3.27}$$

All the energy exchanged through the radial direction in the volume dv is absorbed by the water.

$$Q = \dot{m} \cdot Cp_w \cdot (T_{outlet} - T_{inlet}) \tag{3.28}$$

By replacing the 3.4 in 3.28, we obtained the following relation (valid only for the downward tube and when consider the inner tube adiabatic):

$$\dot{m} \cdot Cp_w \cdot (T_{outlet} - T_{inlet}) = 2 \cdot \pi \cdot r \cdot k_t \cdot (T_v(z) - T_{f,down}) \cdot \Delta z \tag{3.29}$$

Subsequently, we replaced $T_{f,down}$ with the relation reported in 3.27:

$$\dot{m} \cdot Cp_w \cdot (T_{outlet} - T_{inlet}) = 2 \cdot \pi \cdot r \cdot k_t \cdot (T_v(z) - \frac{(T_{inlet} + T_{outlet})}{2}) \cdot \Delta z \tag{3.30}$$

Finally, fixed the T_{inlet}, we obtained an equation where the only unknown parameter is the T_{outlet} so we can calculate it. In detail, fixed a T_{inlet} value of the first volume dv, T_{outlet} of the first volume dv is estimated. This T_{outlet} will became the T_{inlet} parameter of the following volume. This method is implemented from the top to the bottom of the well. From the moment in which the water starts to go up through the inner tube, the heat exchange coefficient changes because now the water is not in contact with the ground but with the downward water. The new equation, obtained by using the equations 3.16 and 3.28, is reported in:

$$\dot{m} \cdot Cp_w \cdot (T_{u,outlet} - T_{u,inlet}) = 2 \cdot \pi \cdot r \cdot k_t \cdot (\frac{(T_{u,inlet} + T_{u,outlet})}{2} - \frac{(T_{u,inlet} + T_{u,outlet})}{2}) \cdot \Delta z \tag{3.31}$$

Also in this case $T_{f,down}$ and $T_{f,up}$ are substituted with the relation reported in 3.27. As now we know all the profile temperature of the downward water, the $T_{f,down}$ is a number and don't contain unknown parameters.
In the first phase of the calculation process, when we are following the downward water for the

first time, we haven't inner tube temperature data available. Therefore, we consider the energy inner tube rate equal to zero (the inner tube is adiabatic).

$$\begin{aligned}\dot{m} \cdot Cp_w \cdot (T_{d,outlet} - T_{d,inlet}) = 2 \cdot \pi \cdot r \cdot k_t \cdot (T_v(z) - \frac{(T_{d,inlet} + T_{d,outlet})}{2}) \cdot \Delta z \\ - 2 \cdot \pi \cdot r \cdot k_t \cdot (\frac{(T_{u,inlet} + T_{u,outlet})}{2} - \frac{(T_{u,inlet} + T_{u,outlet})}{2}) \cdot \Delta z\end{aligned} \tag{3.32}$$

After the first cycle, as now we have a temperature profile of the inner tube, we can recalculate the downward water temperature profile considering the temperature profile previously estimated.
An iterative method is then used to achieve a result with an acceptable error (the obtained profile doesn't change too much because, due to the isolating material used between the tubes, the heat exchange through the inner and the annulus tube is low).
For the evaluation of the friction factor both in the inner tube and in the annulus, and subsequently the calculation of the pressure drops, the Haaland equation was used which models with a function the moody curve in the turbulent regime for rough tubes (therefore taking considering the roughness of the pipes).

$$\frac{1}{\sqrt{f}} = -1.8 \cdot \log[[\frac{\frac{\epsilon}{D}}{3.7}]^{1.11} + \frac{6.9}{Re}] \tag{3.33}$$

Where:

- f is the Darcy friction factor.

- $\frac{\epsilon}{D}$ is the relative roughness.

- Re is the Reynolds number.

3.4 U-tube closed-loop system.

A U-tube geothermal system is composed by two parallel tube connected by a bending at the bottom-hole. The hole between the tubes and the well is filled with grout (usually bentonite), both to prevent the direct leakage between ground and tubes and to avoid the connection between ground and surface.
The grout has to guarantee that the water cannot pass through it, At the same time, it need to have good thermal conductivity to maximize the heat exchange, avoid the passage of mass but allow better passage of heat.

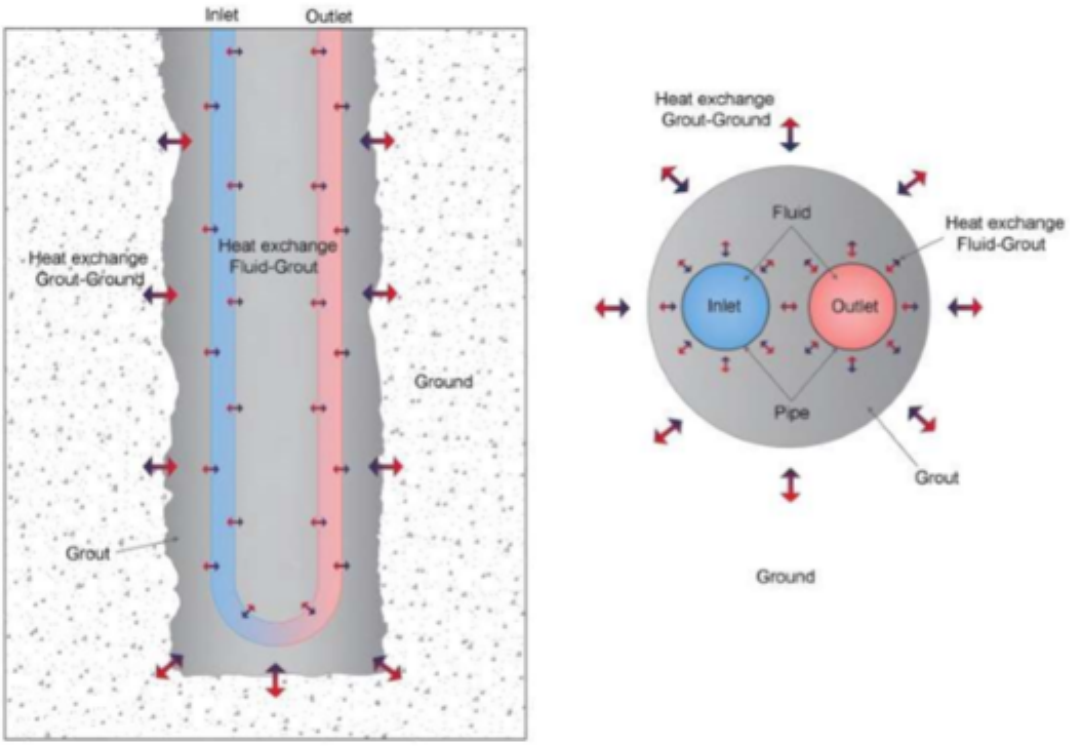

Figure 3.4: Wellbore heat exchange. Cross and schematic sections.

U-Tube thermal resistances.
To compute the temperature profile in the U-tube configuration, by using a one dimensional heat exchange, a model with a set of an equivalent resistances is performed.

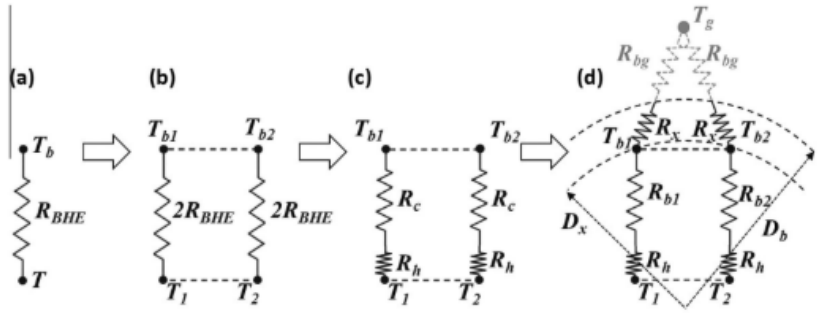

Figure 3.5: Thermal resistances denition steps: (a) borehole resistance, (b) parallel borehole resistances, (c) convective and conductive resistances, and (d) nal resistances conguration.[25]

R_{bhe} represented the thermal resistance between the pipe and the grout node. This parameter is the average thermal resistance among the fluid in the pipe and the borehole wall, and usually it is determined after experimental tests. The grout zone is divided in two zone as the pipe numbers, so also the R_{bhe} is split in two parallel resistances which connect each pipe with the corresponding grout zone. This parameter can be further splited into a convective (R_h) and a conductive (R_c) term.

$$2R_{bhe} = R_h + R_c \tag{3.34}$$

R_c in the previous equation take in account the total conductive resistance between the pipes and the borehole wall.
The gout node will be located at a certain diameter D_x and so R_c is divided in two different resistances.

$$R_c = R_b + R_x \tag{3.35}$$

$$R_b = R_{b1} = R_{b2} \tag{3.36}$$

R_b represent the conductive resistance between the pipe and the node.
The convective parameters R_h can be calculated by the equation:

$$R_h = \frac{1}{\pi \cdot h \cdot D_{p,i} \cdot dz} = \frac{1}{\pi \cdot Nu \cdot \lambda \cdot dz} \tag{3.37}$$

Where:
- $D_{p,i}$ is the internal pipe diameter.
- Nu is the dimensionless number Nusselt.

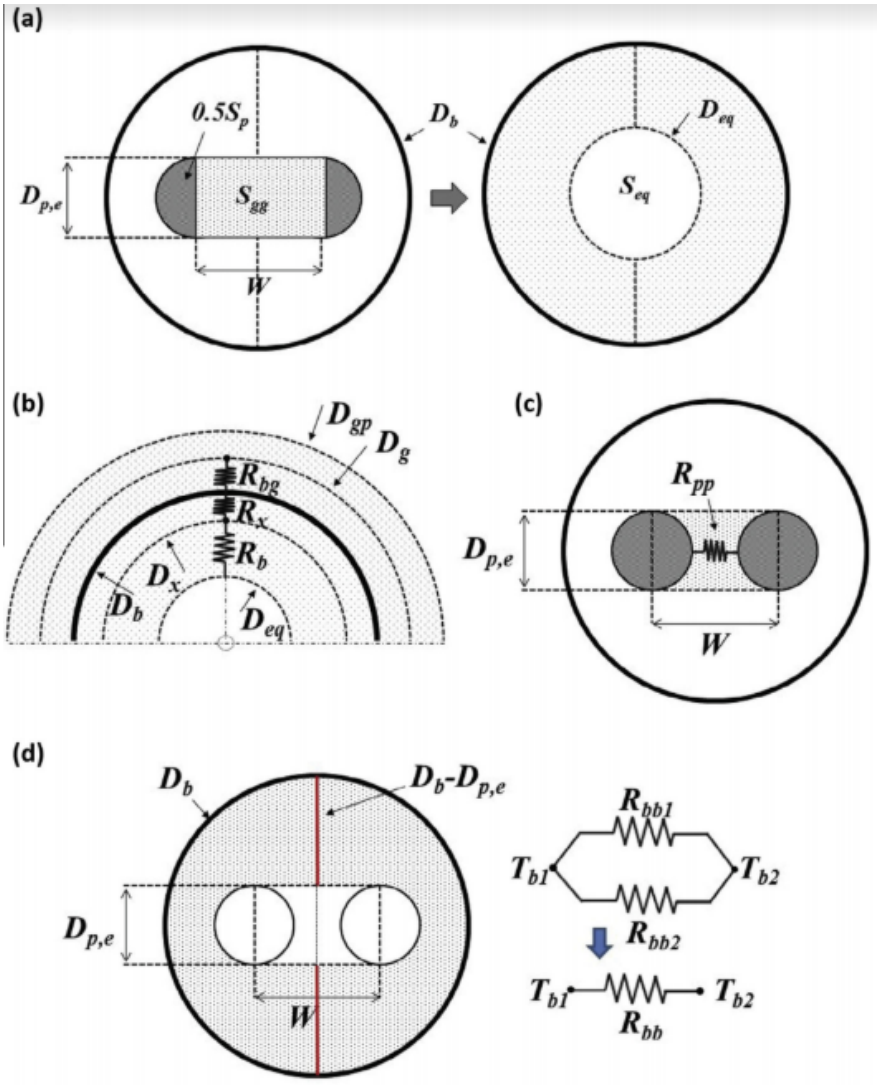

Figure 3.6: Geometrical model characteristics to calculate (a) the equivalent diameter, (b) grout nodes position, (c) pipe to pipe thermal resistance, and (d) grout node to grout node thermal resistance.[25]

Usually the R_{bhe} is calculated through several experimental step-tests, and the different part can be obtained by the tests. But it is possible to estimate thanks to a calculation method with the use of an equivalent surface S_{eq} and its own diameter D_{eq}.

$$D_{eq} = 2 \cdot \sqrt{\frac{S_{eq}}{\pi}} \tag{3.38}$$

The equivalent surface can be estimated in many methods. The approach of Pasquier et al.[26] is used, considering the sum of S_{gg} and S_p, as shown in fig 3.6a. So the equivalent diameter is calculated as:

$$D_{eq} = D_{p,e} \cdot \sqrt{\frac{4 \cdot W}{\pi \cdot D_{p,e}} + 1} \tag{3.39}$$

Now with the equivalent diameter the conductive thermal resistance R_b and R_x are calculated considering a semi-cylindrical conductive heat transfer (eq. 3.40 and 3.41).

$$R_b = R_{b1} = R_{b2} = \frac{\ln\left(D_x/D_{eq}\right)}{\pi \lambda_b dz} \tag{3.40}$$

$$R_x = \frac{\ln\left(D_b/D_x\right)}{\pi \lambda_b dz} \tag{3.41}$$

Where:

-k_b is the grout thermal conductivity.

The internal borehole geometry, overall the u-tube pipe positions like spank spacing and distance pipes-borehole wall, influences the D_x position. Usually, when the pipes are near to the borehole wall, D_x can be located ad the same distance of the borehole wall, so D_x=D_b. So the R_x part of the conductive resistance can be neglected.
To simplify the problem and so the model the resistances between the grout nodes (R_{bb}) and the two pipes (R_{pp}) are neglected.
So the model give us an overestimation in the output temperature and not the real profile temperature, but our interest is to show that the u-tube technology has a lower output temperature and efficiency performance than the coaxial heat exchanger.
For the estimation of the ground thermal resistance is used the correlation 3.8.
The total resistance for the single tube is:

$$R_t = R_h + R_b + R_x + R_s \cdot \frac{D_w}{\frac{1}{2} \cdot D_w \cdot \pi dz} \tag{3.42}$$

This includes convective (R_h), grout conduction ($R_b + R_x$) and ground resistance (R_s) part.

4. Open-loop geothermal energy systems

4.1 Open loop systems

In different studies of the past years, authors were oriented in the direction of the implementation of open loop systems by using directly oil or gas reservoir as a geothermal reservoir.
An open-loop system consists at least in an injection and an extraction well. A fluid is pumped through the injection well into a reservoir, where it gains heat from surrounding rocks before it is circulated through an extraction well.
Due to the direct use of the aquifer water, in open-loop systems some hydrochemical problems usually can occur [27]:

- particles in the water may clog or abrade the heat exchanger.
- minerals such as calcite or iron oxyhydroxide may precipitate.
- If the groundwater is saline enough, reducing enough or contains enough dissolved gases (CO2, H2S), it may promote corrosion.
- The groundwater circulation may promote the formation of biofilms: slimes of non-pathogenic bacteria, that are commonly found in the geological environment. These biofilms can clog up well screens, pipes or heat exchange elements.

Scaling and corrosion phenomena are also frequent, both in reinjection wells and in production ones. These phenomena are related to the chemical composition of the brine, the pH value, the pressure and temperature changes and the over-saturation of some dissolved minerals. Corrosion and scaling can cause the damages to pipes, the reduction of casings diameters and so an efficiency decrease of the geothermal well.
Maintenance operations and additional costs will be necessary.
Another common problem is represented by the way to dispose the wastewater. Usually the following options for water disposal are used [27]:

- Disposal to a surface waterbody;
- Re-injection to the abstracted aquifer;
- Disposal to another aquifer;
- Disposal of wastewater to the abstraction well;
- Disposal to sewer.

The purposes of the different reinjection procedure are different: to reinject in the underground the fluids that have physicochemical properties not suitable to the terrestrial ecosystems; to avoid the depletion of the geothermal reservoir gathering in the underground the produced brine; to re-establishing the underground pressure; to offset surface subsidence caused by the pressure decline due to the production.
Reinjection operations entail high economic costs since they require the drilling and/or maintenance of additional wells, the treatment and the pumping of the fluids.
Reinjection entails also some risks the injected cold water could interfere with the hot waters of the production level often because of "short-circuiting" along direct flow-paths such as open fractures, the geothermal fluids could pollute the groundwater, the corrosion and scaling in surface pipelines and in the reinjection wells, the seismicity phenomena.

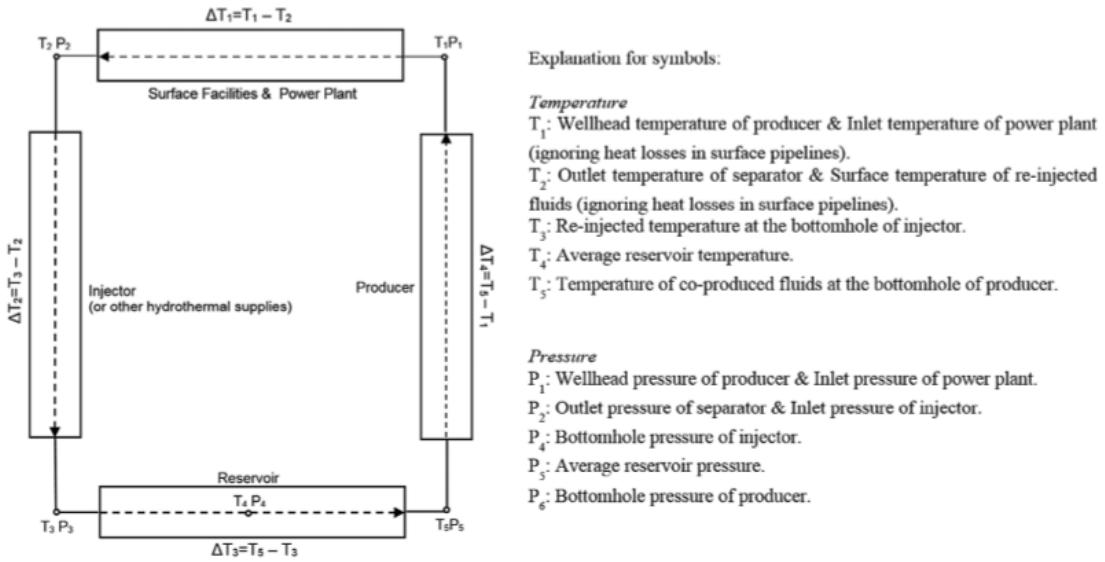

Figure 4.1: Simplied scheme for geothermal energy recovery from hydrocarbon systems.[28]

Figure 4.1 shows a basic framework consisting of four components: Surface facilities and power plat, injector, reservoir and producer.
In oil and gas mature fields when extracted the fluid from the reservoir an amount of hydrocarbons is present in the fluid, usually is more convenient to separate it from the water before the inlet in the power plant. After the co-produced fluids are separated at the separator, the disposed water is re-injected underground via the injector. In this process the injected water is heated by surrounding rock because the temperature differential between water and formation. So the injected temperature will be lower then the temperature at the bottomhole.
For water sources of a mature field, two different scenarios may happen:

- Weak natural water drive with partial water injection (such as a mature field with a long time water flooding history).

- Strong natural water drive with no water injection (such as a mature field with powerful aquifers).

The injected water, reached the bottom, spreads in the reservoir, and in doing so extract heat.
One indicator of the stored heat in the underground, is the average reservoir temperature [28].

4.2 Projects worldwide

The idea to exploit and retrofit hydrocarbon production wells to extract heat is relatively novel, only a few studies have been successfully carried out in the last years.
To prove the feasibility of harnessing heat from mature oil and gas field two case studies are reviewed.
Two pilot projects with power unit have been installed in Naval Petroleum Reserve (USA) and in Huabei (China) oil fields [28].

4.2.1 Naval Petroleum Reserve NO.3, Wyoming, USA

The exploitation started in the early 1920's, after which it was shut-in for a relatively long time. In 1976, Naval Petroleum Reserve NO.3 field was fully developed. Its have a very interesting parameters, such as the reservoir temperature (around 110C) and the geothermal gradient (25C per Km). In the oil production a large amount of hot water is created with a temperature of around 80-90C, from more than 700 active wells. the water supply is guaranteed by the Big Horn Range, located in the northwest of the field, with a 2438m hydraulic head above the field's surface [29].
In 2007, Department of Energy decided to employ Naval Petroleum Reserve NO.3 field as a demonstration site for low-temperature geothermal energy recovery, due to increasing operational cost and declining oil production.
To exploit the hot co-produced water in August 2008 a 250 kW Organic Rankine Cycle (ORC) was installed. In the following years improvements were made to the plant to minimize the heat loss and improve efficiency. Until the beginning of 2011, the ORC unit produced more than 1900 MWh [30].
In 2015, the plant was sold to a private company.

Table 4.1: Historical milestones of Naval Petroleum Reserve NO.3.[28]

Years	Milestones
1920	Production started
1976	Fully developed at field level
2000	Oil production declined
2007	Employed as a demostration site for geothermal energy extraction
2008	250kW ORC power plant installed
2011	Cumulative electrical output of over 1900MWh
2014	Sold to a private company

4.2.2 Huabei oil field, Hebei, China

The Huabei oil field, owned by China National Petroleum Corporation (CNPC), is located in the Hebei province of northern China. it was one of the most productive field in the nation, for around 15 years after its discovery.
There are 27 existing wells in place and only 6 of them are production wells. the flow rate has declined from 700 to 150 $\frac{m^3}{day}$, after more than 30 years of water flooding [31]. The reservoir temperature is about 120C and the geothermal gradient in the zone is 35C for km. The water cut increased up to 97% [32] and in 2007 CNPC conducted a pilot test to harness geothermal energy from the LB reservoir.
In 2011, a 400 kW binary power generator was installed, this is the first heat-electricity unit that exploit low-enthalpy energy from co-produced fluids in oil and gas field in China. The temperature of the fluid in surface is around 110Cand the flow rate from 8 well is 2880 $\frac{m^3}{day}$. Until the end of 2011, the operation time is 2880h and the electrical energy produced was around 31X10^4 kWh [32].

Table 4.2: Historical milestones of Huabei oil field.[28]

Years	State points
1975	Discovered
1976	Production started
1986	Oil production declined
2007	Employed as a pilot site for geothermal energy extraction
Early April 2011	400kW binary power plant installed
End of 2011	Cumulative electrical output of over 310MWh

4.3 Open loop oil and gas heat recovery potential

Many studies have been carried out in several oil and gas fields worldwide to calculate the heat recovery potential.
For example, in the Gulf Coast fields can be generated over 1 GW of electric power according to Mckenna et al.[33]. Limpasurat et al. [34] studied the opportunity to exploit the heat accumulated in heavy oil fields that have undergone steam flooding and esteemed that the net power generation from a injection-producer system could be around 14 kW.
In the Los Angeles area the net energy output from oilfields could be around 7430 kW [35], with a net present value after 30 years of 41 million dollars. Instead in the U.S. Gulf Coast the net geothermal power from coproduced fluids could be around 350 kW [36].

4.4 Important parameters to select suitable candidates

There are some parameters, that falling in certain range, determine a good field for the exploitation of geothermal recovery heat and give us a criteria to define a suitable candidate for an open loop system[28].

Flow rate

The flow rate extractable from a well or a field depend on the area. But high production flow rate are recommended, as confirmed in the pilot project in the area of Hebei in China, for the generation of geothermal power from a resource with low to medium temperature water.
High flow rate allow to exploit more power from a no high temperature resource and integrate it with a electric or district heating power plant.

Wellhead temperature

The wellhead temperature is an important parameter to select the appropriate technology to make the most of the removed thermal power. As a general criterion, it should be at least higher than the minimum temperature required for the power plant, for the direct use it depends on the application and for the electric generation it depend on the kind of ORC utilized.

Water cut

The water cut is the ratio of water produced compared to the volume of total liquids produced from an oil well. Mature oil and gas fields are characterized by high water cut and so they are a good candidates for this type of application.
Most mature fields require long-term, stable water supply, such as water injection or natural fluid recharge at the reservoir boundaries to sustain hydrocarbon production.

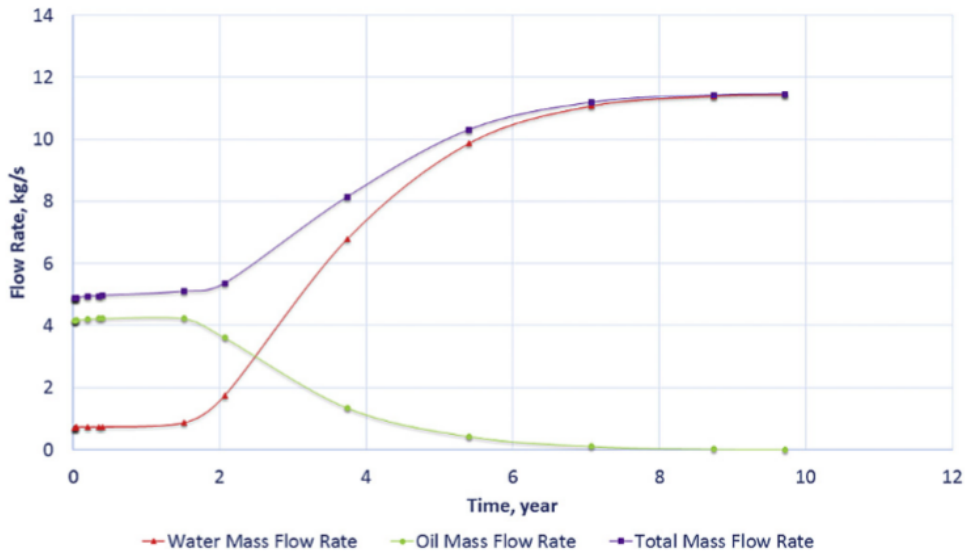

Figure 4.2: Water and oil flow rates over time.[28]

Average reservoir temperature and geothermal gradient

Average reservoir temperature is a good indicator of stored heat in subsurface and it increase with depth, the rate of growing depend on location, each location has an own geothermal gradient. Geothermal gradient is the rate of increasing temperature with respect to increasing depth in Earth's interior.

Usually, for this type of application, the average reservoir temperature varies from 100C to 200C, lower temperature may not be suitable for heat recovery.

With a rough calculation, the temperature of the reservoir can be calculated by multiplying the geothermal gradient by the depth of the formation.

Permeability and porosity

Permeability is the property that indicates the ability for fluids to flow through porous media. High permeability will allow fluids to move rapidly through rocks so it partly controls how much heat can be transferred through the formation to the produced fluids by means of convection. permeability depends strongly on the geological formation.

Flow in porous media can be enhanced by natural fracture networks which are additional channels. Porosity is defined as the ratio between the pore volume and the total volume of the rock. It is useful to estimate the amount of fluid can be stored in the reservoir and with the average temperature the energy stored can be calculated.

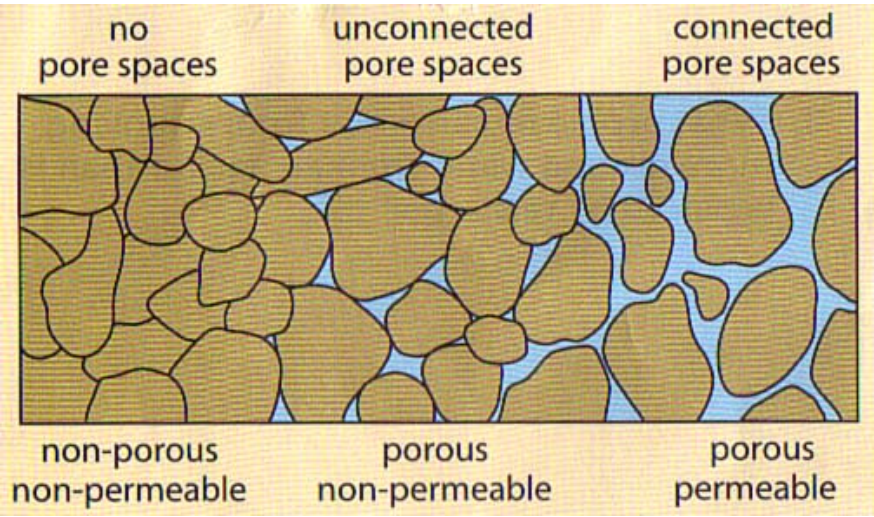

Figure 4.3: Porosity and permeability correlations [37]

Water flooding and steam flooding

After a first period of extraction, to improve the hydrocarbon spill, a water flooding of the reservoir is performed in most of the fields (figure 4.5). It can complement reservoir pressure effectively and, at the same time, create sizable water volume underground. The water in the reservoir can become the thermo-vector fluid for geothermal energy.

Another method to improve the oil extraction is the steam flooding (figure 4.4). It, with a high temperature, decrease the oil viscosity so favouring oil flowing but also release a considerable waste heat in the subsurface. This energy can be recovered by this type of system.

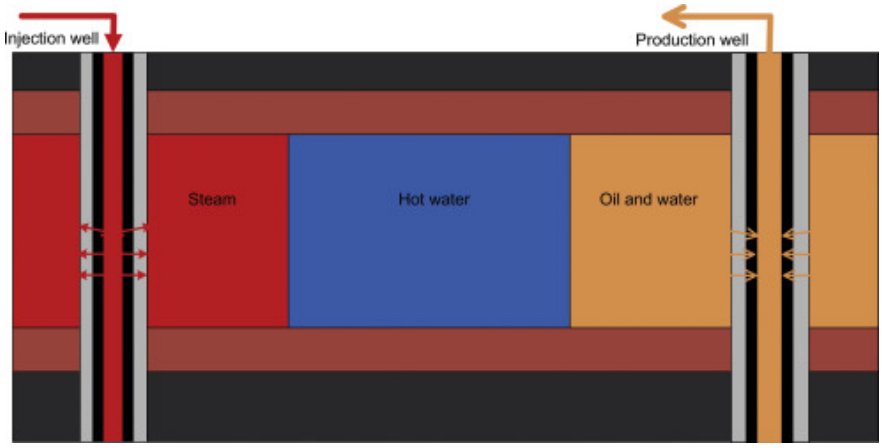

Figure 4.4: Steam flooding [38]

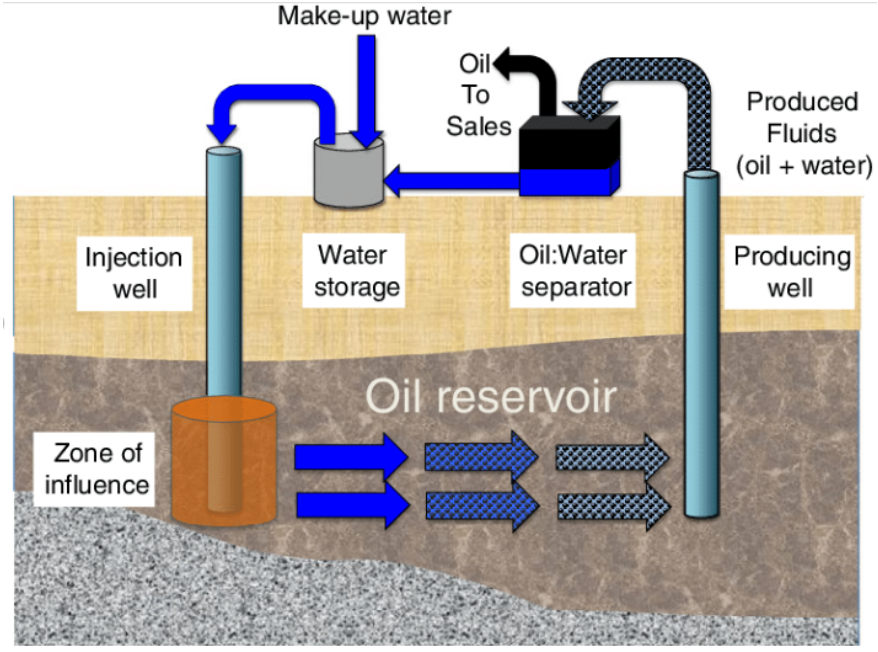

Figure 4.5: Water flooding [39]

Type of power plant

All the outlet parameters must to fit with the final use of the heat recovered. the final use can be direct (figure 4.6) or indirect use. Very popular is the use of an Organic Rankine Cycle (figure 4.7) to produce electricity with a low-medium temperature heat, using specific process fluids. The normal Rankine Cycle is not suitable for the low temperature of the water taken out and so a specific fluid is used depending on the temperature of the heat extracted.

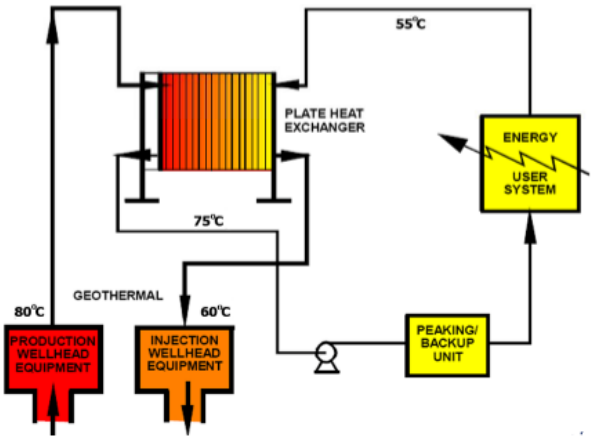

Figure 4.6: Typical direct use geothermal heating system configuration.

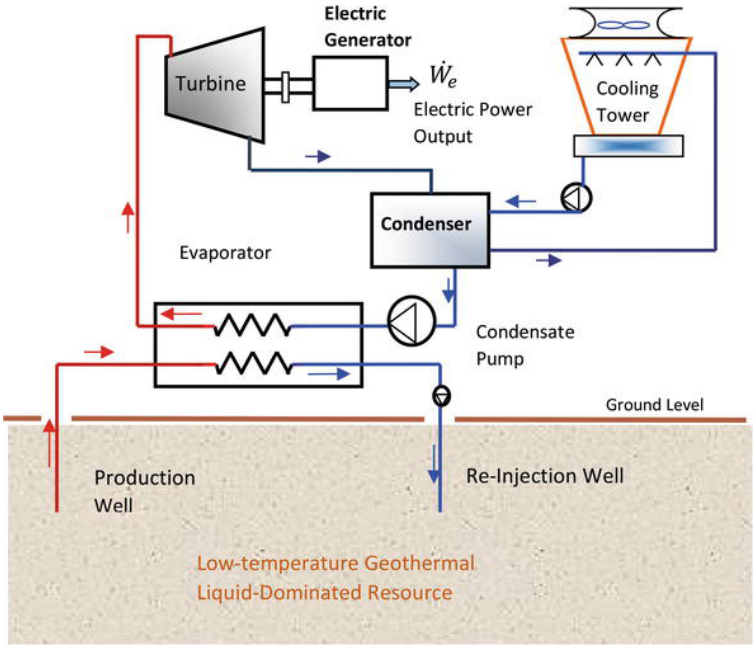

Figure 4.7: ORC-Based Geothermal Power Generation [40].

4.5 Open loop oil and gas well model

Also in this case a model is performed to evaluate the temperature profile in the extraction well and also to compute the heat power exploited. The thesis work is centred to the closed loop systems and a study on open loop systems is done only to have a more points of view to evaluate in a better way the pros and cons of a closed loop system.
The temperature profile of the produced fluid along the wellbore depends on thermal property of fluid and surrounding rocks, wellbore configuration, flow rate and time.
In this work all the calculation is done under the steady state assumption.
The ground resistance is computed, as in the u-tube and coaxial heat exchanger, by the eq 3.8. The convective resistance associated with the fluid flow in the pipe is estimated through the dimensionless Nusselt number.

$$h = \frac{Nu \cdot \lambda_f}{2r_w} \tag{4.1}$$

where:

-r_w is the radius of the tube.

-h is the convective heat transfer coefficient.

The Nusselt number can be evaluated, assuming turbulent flow inside the tube, as

$$Nu = 0.023 \cdot Re^{0.8} \cdot Pr^{0.4} \tag{4.2}$$

Where:

$$Pr = \frac{Cp \cdot \mu}{\lambda} \tag{4.3}$$

$$Re = \frac{\rho \cdot v \cdot D}{\mu} \tag{4.4}$$

The resistance associated to the thickness of the tube is neglected,due to the high thermal conductivity of the steel piping.

So the total associated resistance is :

$$R_t = D_w \cdot R_s + \frac{1}{h} \tag{4.5}$$

The input temperature in the model is the temperature at the bottomhole of the well, it is then assumed as the temperature of the reservoir. The reservoir temperature can be calculated, in a simplify method, as the average geothermic gradient of the zone multiplied by the length of the well.

$$T_{bottomhole} = L_{well} \cdot \frac{dT}{dz} \tag{4.6}$$

Where:

-L_{well} is the depth of the well.

-$\frac{dT}{dz}$ is the average geothermal gradient, usually the value is from 20 to 35 $\frac{C}{km}$ if geothermal anomalies not occur.

5. Results

5.1 Constant ground properties

In all the profile temperature for each configuration, in a previous analysis, the properties of the ground are kept constant for the entire length of the well (λ 2.5 $\frac{W}{m \cdot K}$, ρ_s 2600 $\frac{kg}{m^3}$ and c_p 800 $\frac{J}{kg \cdot K}$) and the inlet temperature of the fluid equal to 85C.
In the case of open loop no inlet fluid temperature exists, because we take in consideration only the production well.

5.1.1 Coaxial closed loop configuration

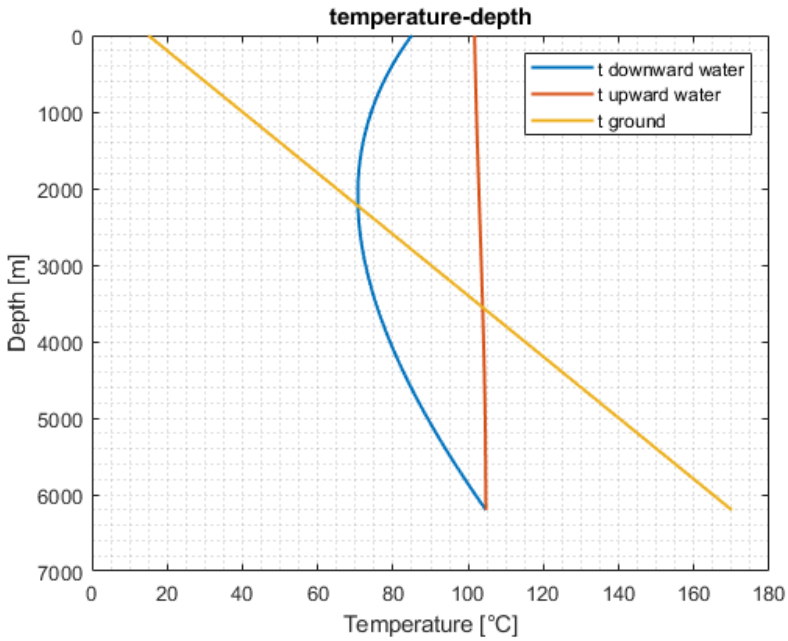

Figure 5.1: Profile temperature in the coaxial configuration

In the first 2000m, during the descent of the fluid, the thermo-vector decrease its temperature. The downward fluid is in thermal contact with the ground at one side and with the upward tube to the other side. In the first section of the pipe, the ground give a negative contribution instead the inner tube positive. The negative contribution is larger and so the water temperature is reduced but when

the water and the ground temperature are close the negative contribution is very low so an increase of water temperature occurs also when the surrounding ground has a lower temperature.
Otherwise, when the downward water profile line crosses the ground temperature line the real heating process of the ground begin, the power ground part became positive. The main aim for the increasing of the temperature is due by the ground because the heat exchange coefficient between the anulus and the inner tube is very low due to the presence of insulating material, it guarantees a higher wellhead temperature.

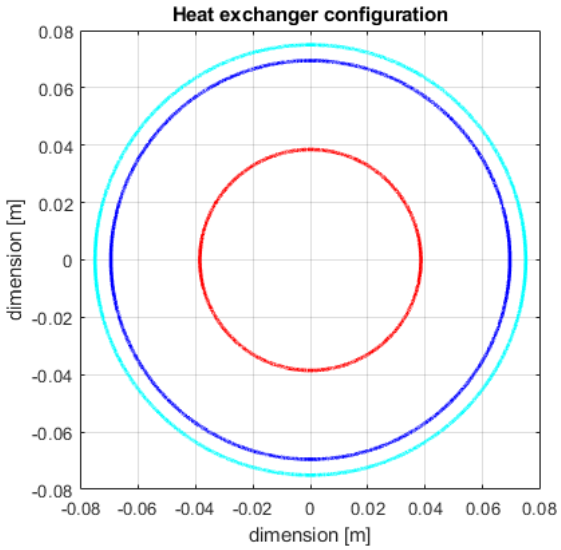

Figure 5.2: Heat exchanger geometry

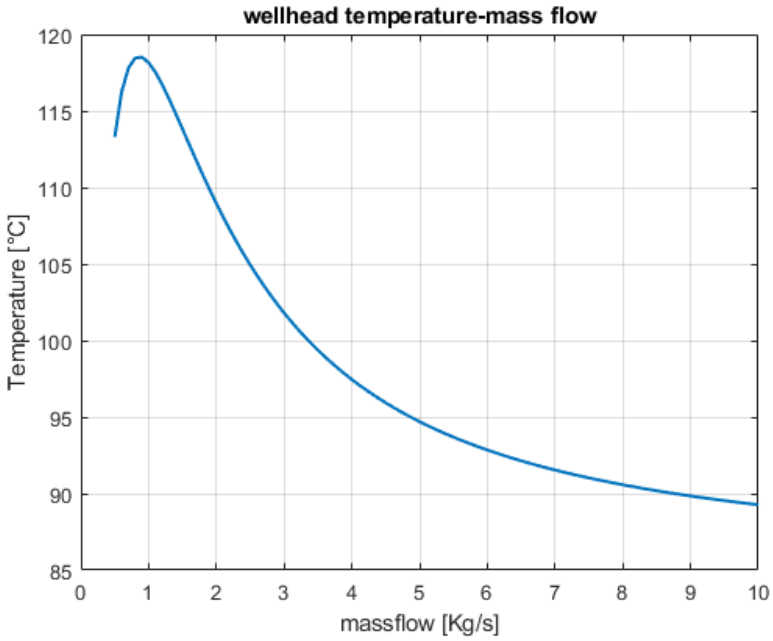

Figure 5.3: Wellhead temperature behavior when the mass flow rate changes

This is the wellhead behavior changing the mass flow rate, as can be seen from 0.5 up to about

0.8 $\frac{kg}{s}$ the output temperature increase up to about 118C then the trend is inverted. So a mass flow rate exists to optimize the wellhead temperature.

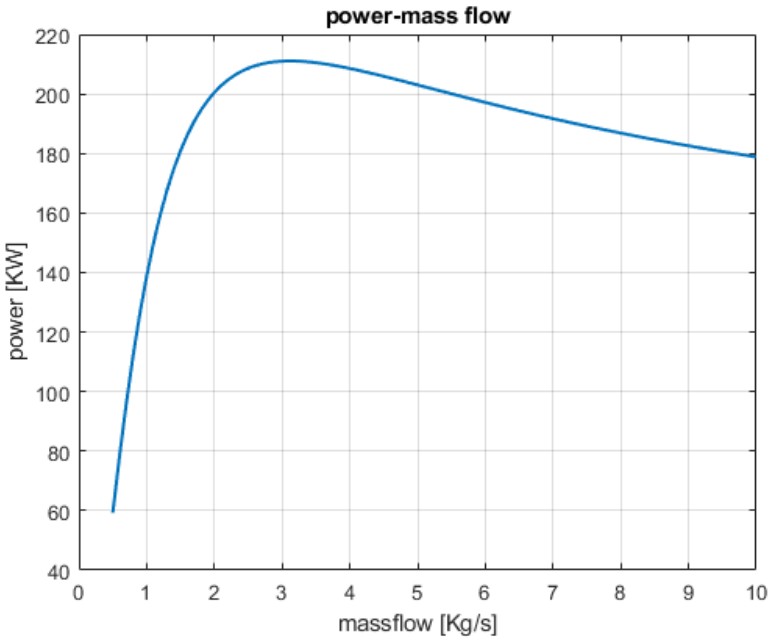

Figure 5.4: Power behavior when the mass flow rate changes

The mass flow rate that maximizes the power extracted doesn't coincide with that which maximizes the exit temperature from the well.

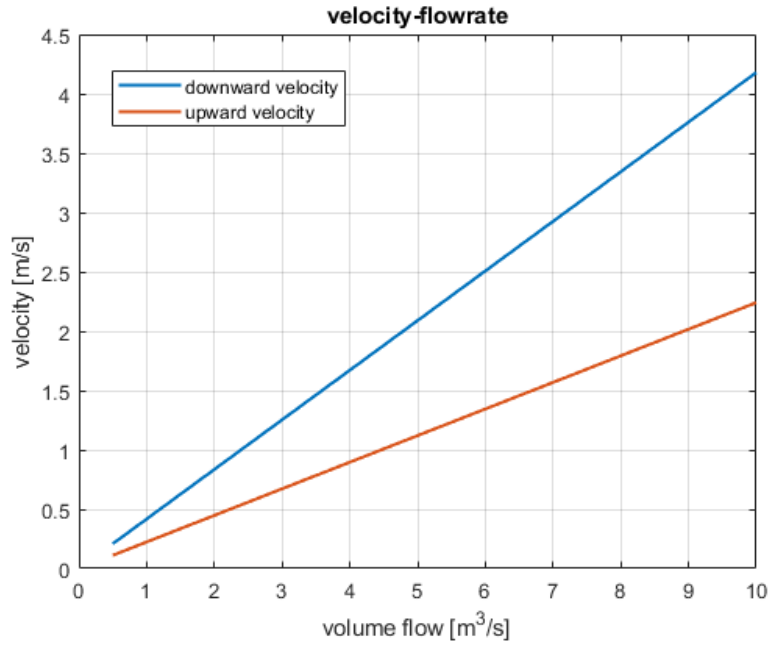

Figure 5.5: Velocity in anulus and inner tube when the mass flow rate changes

It is very important also take in account the pumping cost, and so the head losses in the pipes.

The pressure loss is calculated by the eq. 3.20, as can be seen, the losses are proportional to the second power of the velocity, so an increase in the mass flow causes an increase in the losses.

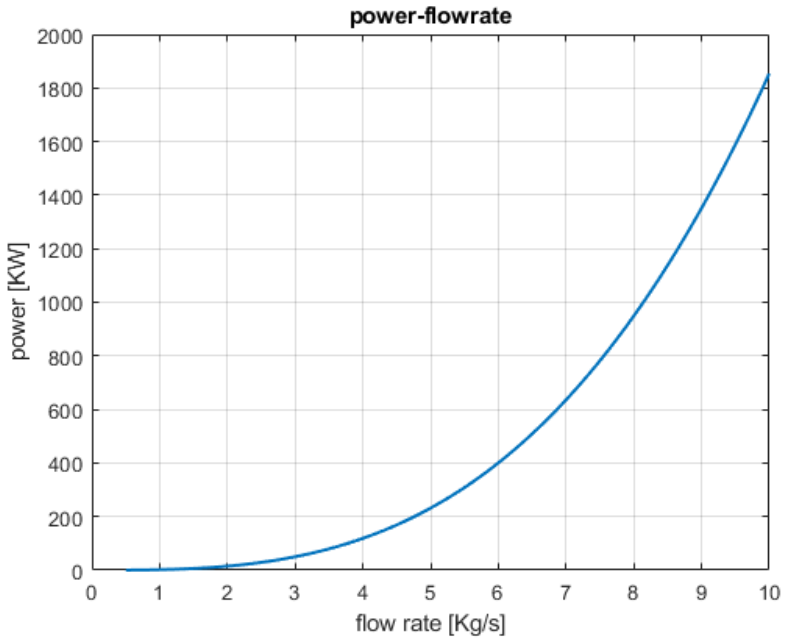

Figure 5.6: Pumping power behavior when the mass flow rate changes

5.1.2 U-tube closed loop configuration

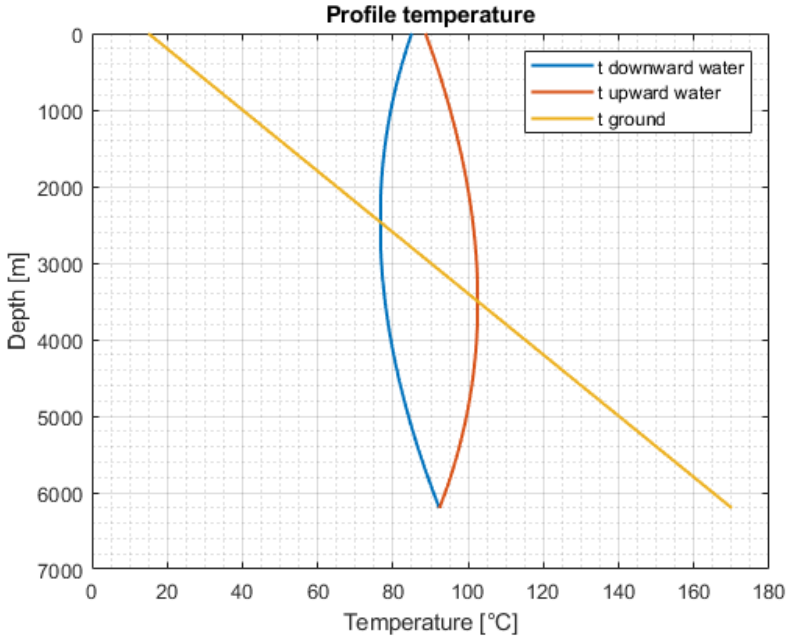

Figure 5.7: Profile temperature in the U-tube configuration

This is a characteristic pattern of the U-tube profile temperature. In this configuration the ground uses large temperature variations both in the descent tube and in the ascent tube.
In the first part, up to near 2500m, the fluid is cooled by the ground. After, when the temperature profile line crosses the ground profile line, the trend is inverted and the carrier fluid begins to increase its temperature. This happens up to the second cross of the fluid line with the ground line, from this point the fluid is cooled up to the surface.
So many heat losses occur also in the upward tube, the pipe releases part of the heat previously accumulated thank to the higher temperature of the subsoil.

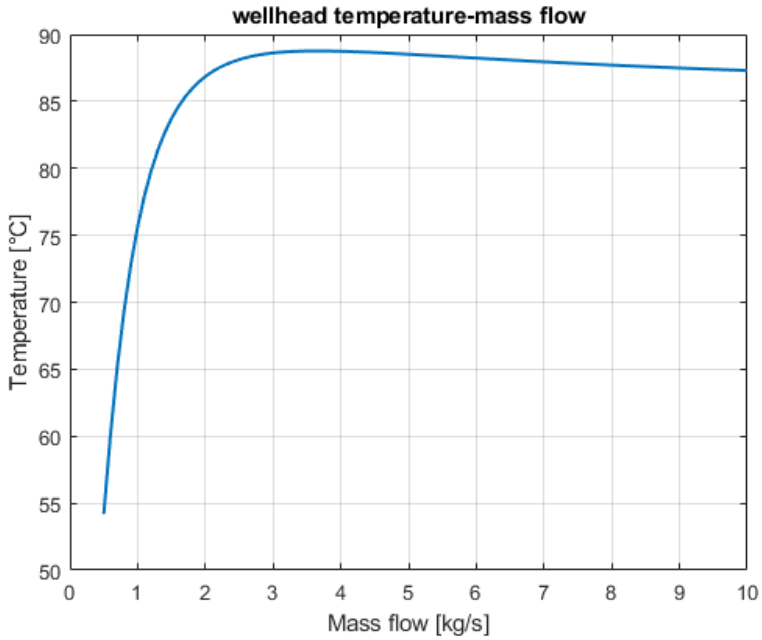

Figure 5.8: Wellhead temperature behavior when the mass flow rate changes

The figure 5.8 shows how the wellhead temperature changes in dependent on mass flow. Up to a mass flow of 1.7 [$\frac{kg}{s}$] the fluid arrives to the surface cooler than the input temperature. So under this value of mass flow there aren't useful effects, if our goal is to heating the fluid. Above this value the output temperature is higher than the input with a maximum between 3 to 4 [$\frac{kg}{s}$].

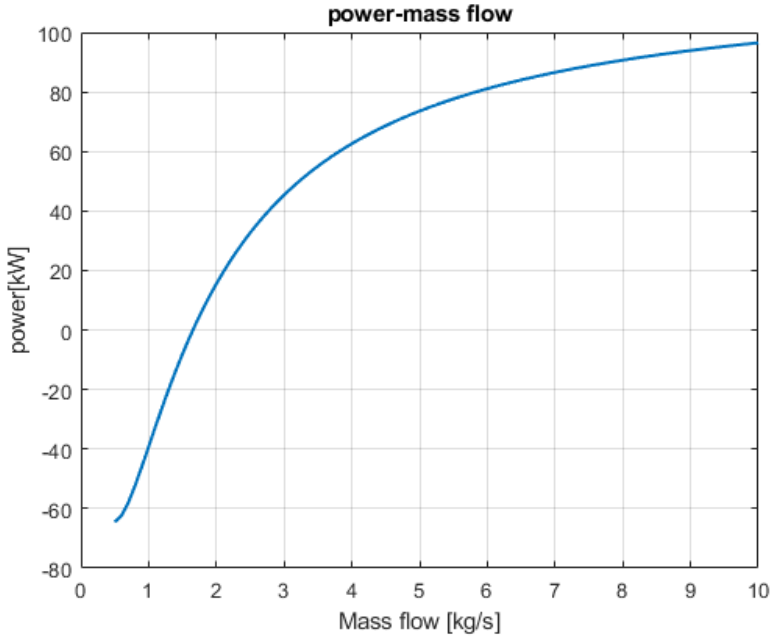

Figure 5.9: Power U-tube behavior when the mass flow rate changes

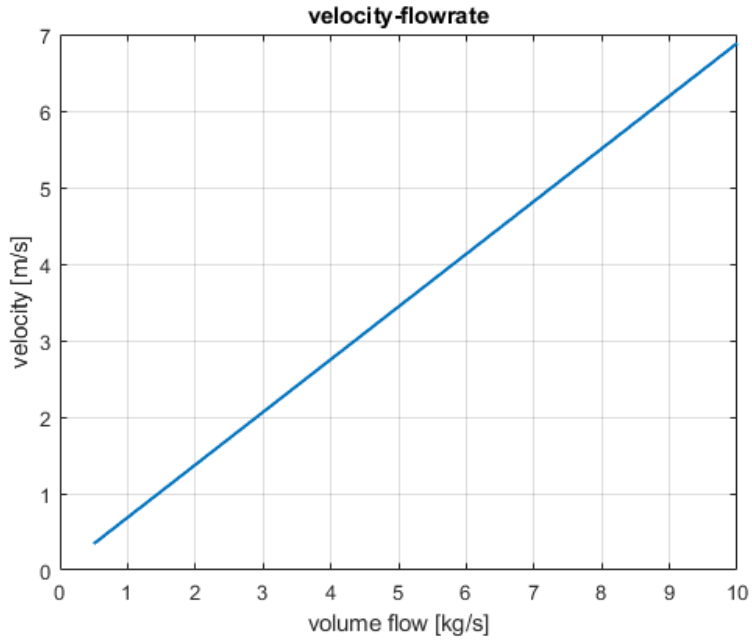

Figure 5.10: Velocity in U-tube when the mass flow rate changes

The velocity in the U-tube pipes grow directly proportional to the mass flow. In this case, fixed a mass flow value, there is only a velocity because in this configuration there aren't change in the area along the pipes.

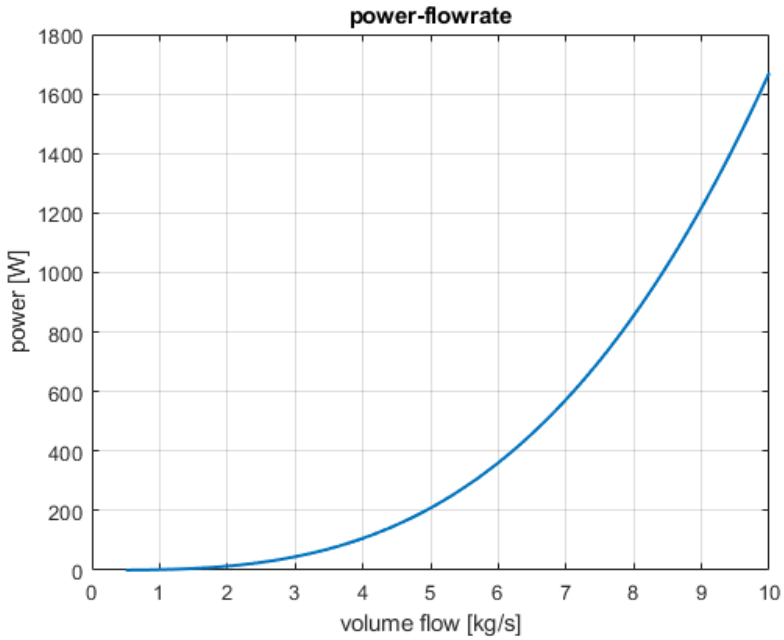

Figure 5.11: Pumping power behavior when the mass flow rate changes

5.1.3 Open loop configuration

The fluid start to be extracted from the bottomhole, so the starting data is the fluid temperature at the bottom and then it pass trough the pipe up to the surface.
A common profile temperature of this technology is represented in the figure below.

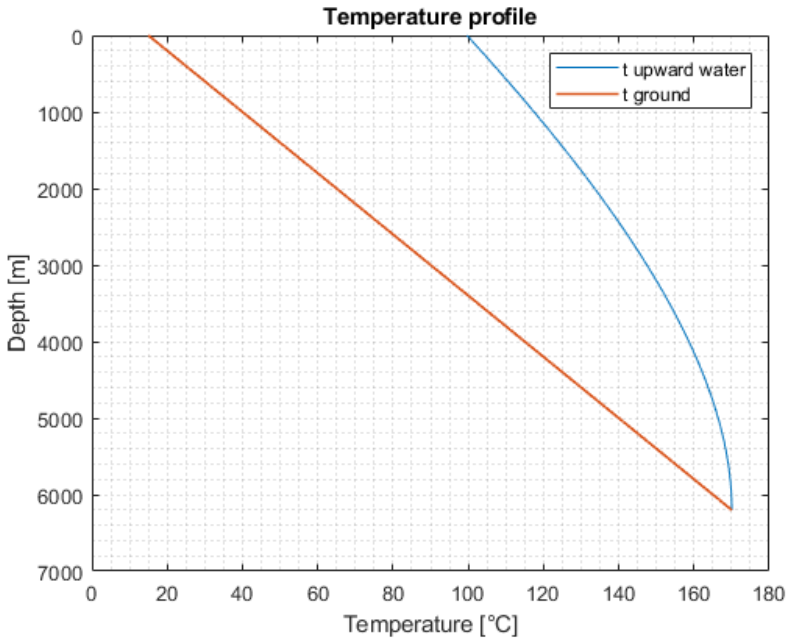

Figure 5.12: Profile temperature in open loop configuration

The fluid in the ascent always disperses heat until it exits the well. The fluid lost heat because the ground is for the all depth always at a lower temperature than the fluid temperature.

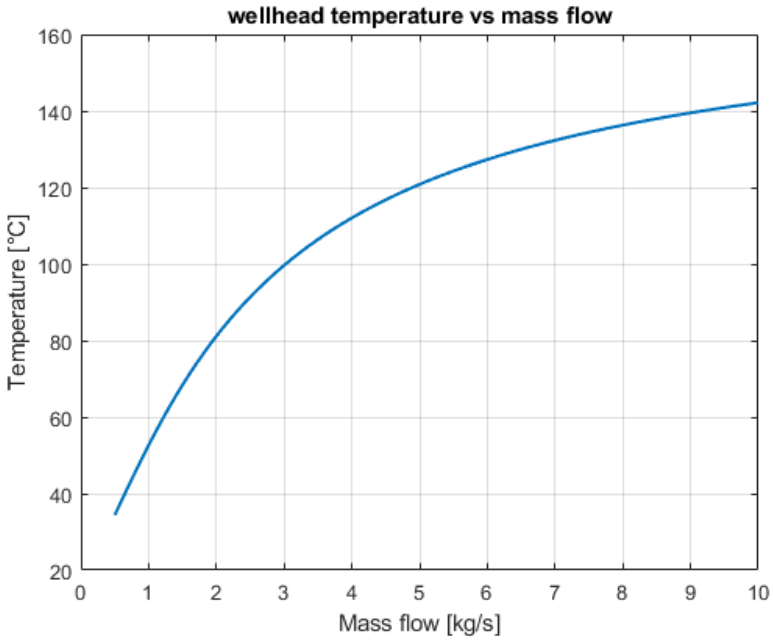

Figure 5.13: Wellhead open loop temperature by varying Mass flow

As can be seen from the figure 5.13, an increase of the mass flow causes an increase in the wellhead temperature. A major velocity in the pipe guarantees a lower heat dispersion keeping the fluid warmer.

5.2 Ground properties dependent on depth

Many studies have been done to understand if the properties of the soil could have significantly influenced the output of the model. Sensitivity analysis has been very useful to comprehend the variation of the output changing the input data of the ground properties.

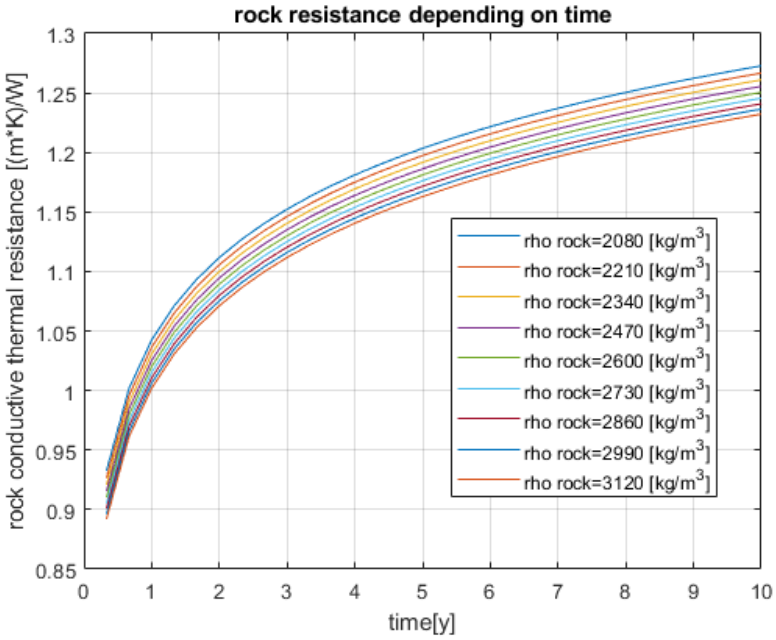

Figure 5.14: Soil resistance over time with different ground density

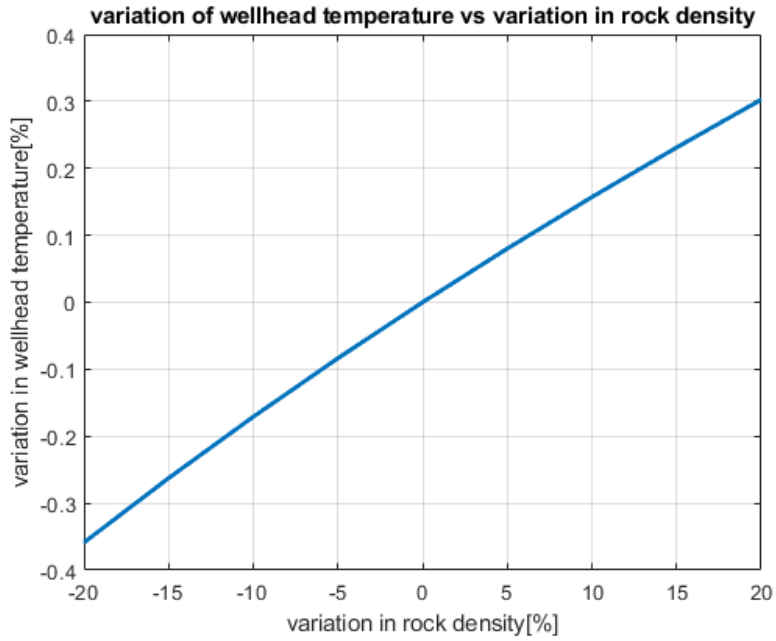

Figure 5.15: Percentage alteration wellhead of temperature with variation of density

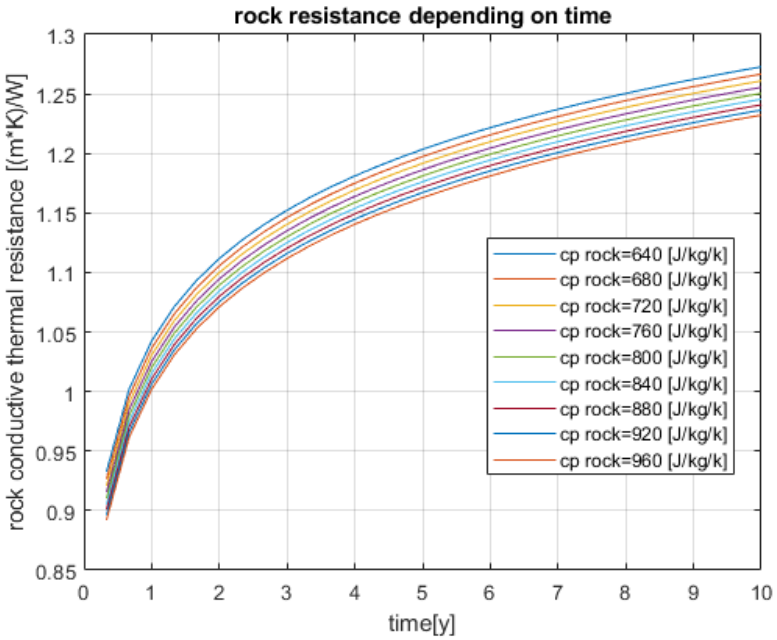

Figure 5.16: Soil resistance over time with different ground specific heat

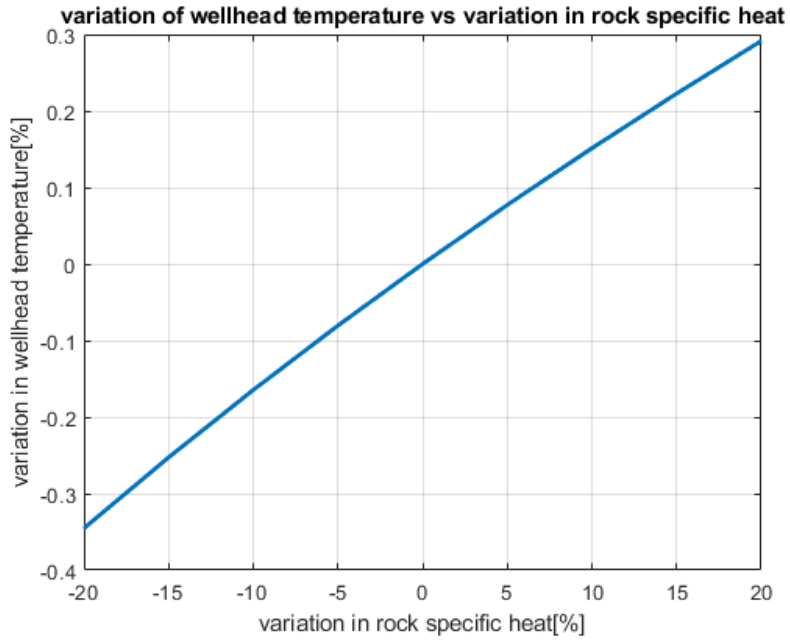

Figure 5.17: Percentage alteration of wellhead temperature with variation of specific heat

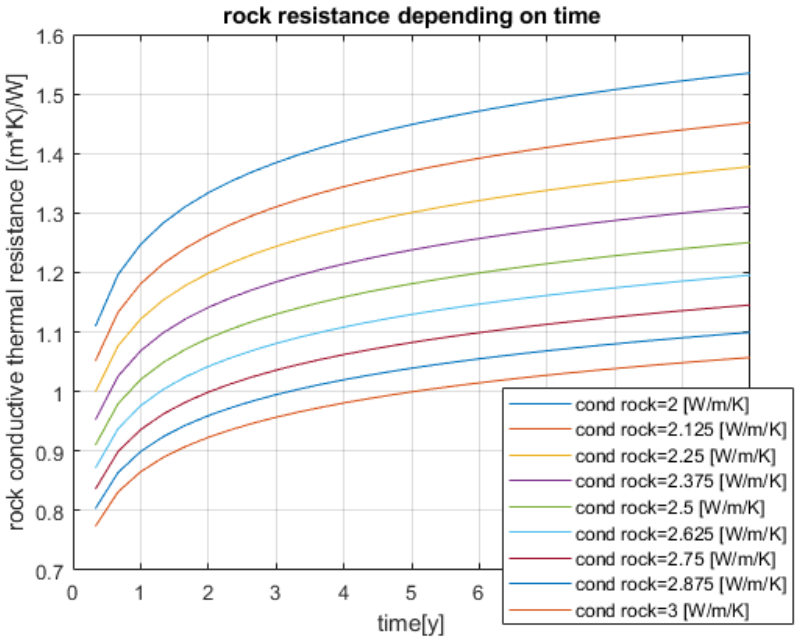

Figure 5.18: Soil resistance over time with different ground conductivity

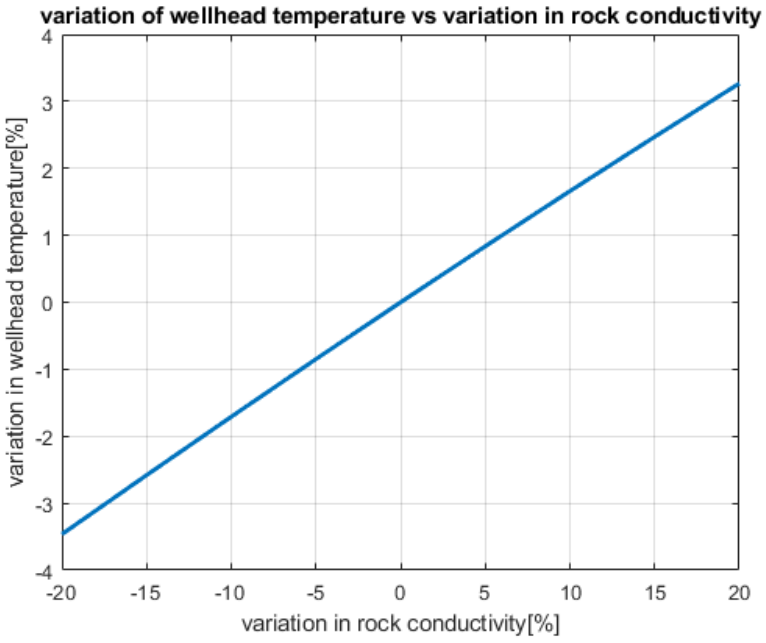

Figure 5.19: Percentage alteration of wellhead temperature with variation of conductivity

As can be seen in the fig 5.15 5.17 5.19 the outlet temperature can be modified by the ground properties by a few percentage points. The ground property that causes the greatest wellhead temperature variation is conductivity. The properties influence directly the ground resistance as highlighted in the eq. 3.8.
Therefore a choice to apply a simplified stratigraphy of the analysed area was considered in the model.

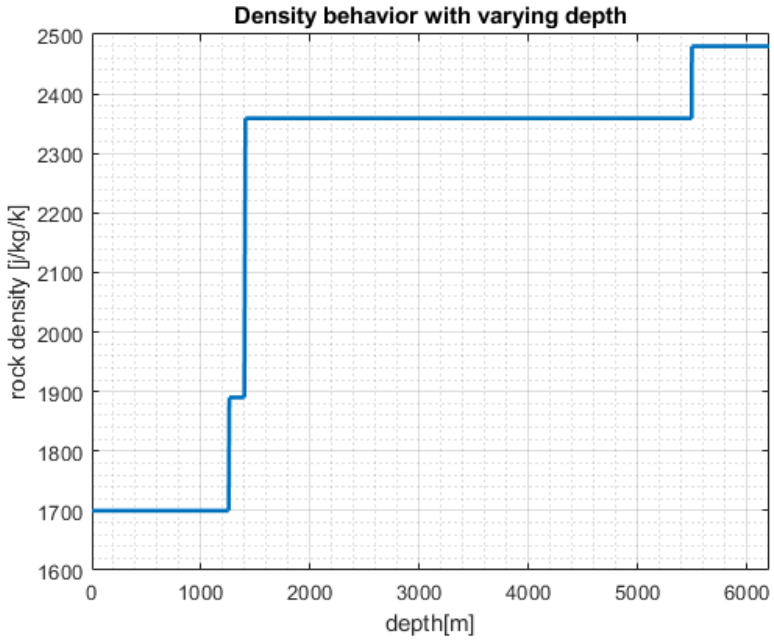

Figure 5.20: Rock density profile used in the model.

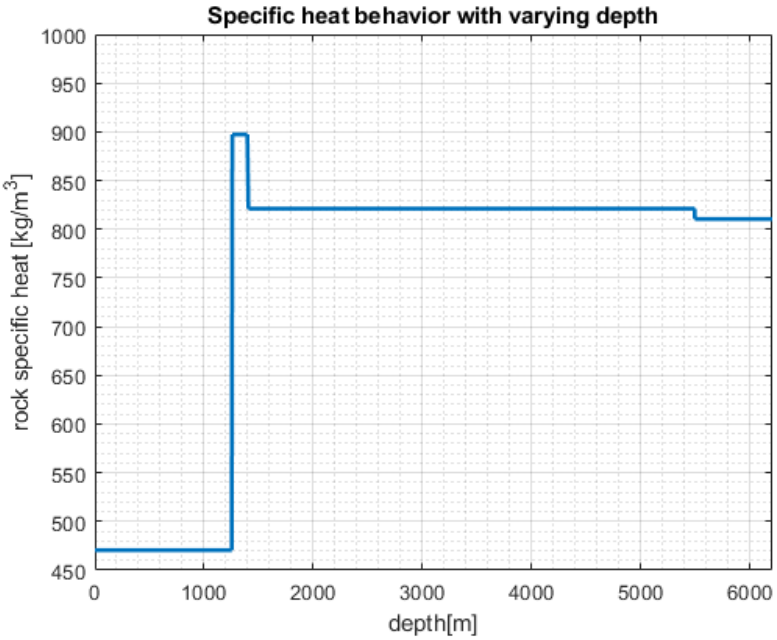

Figure 5.21: Rock specific heat profile used in the model.

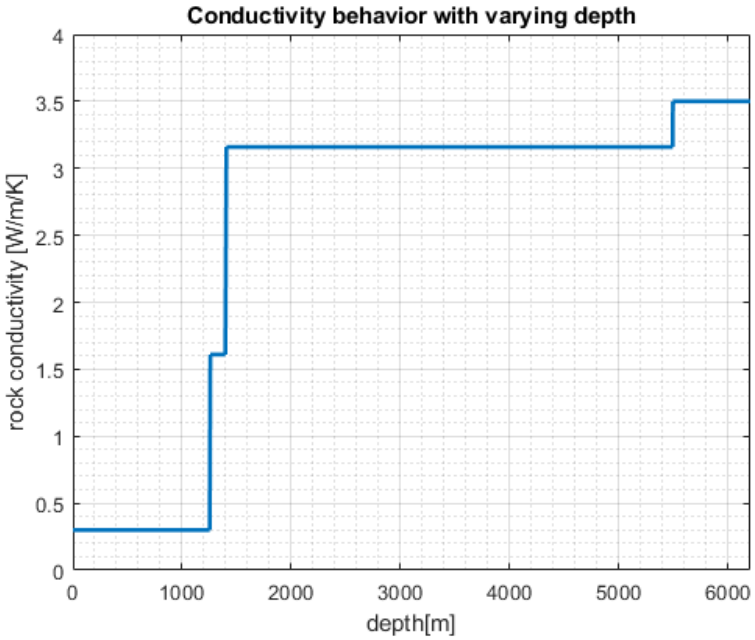

Figure 5.22: Rock conductivity profile used in the model.

5.2.1 Coaxial closed loop configuration

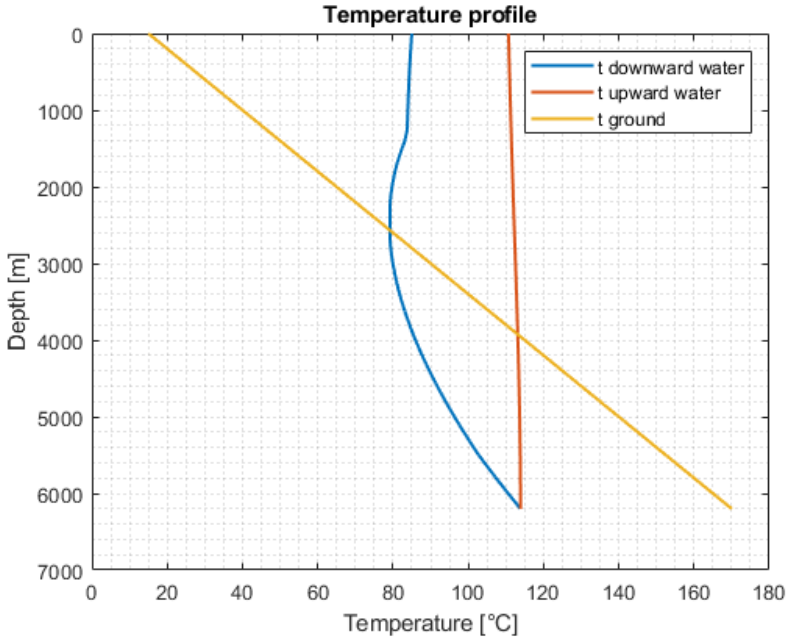

Figure 5.23: Profile temperature in the coaxial configuration taking into account stratigraphy

In the Coaxial configuration the fluid is cooled for the first 2600m, this value is higher than in the constant ground model because the fluid is kept warmer so the the match of the fluid and ground temperature occur at an higher depth. After this depth the fluid is heated up to the bottom. The stratigraphy applied to the model improve the wellhead temperature in the coaxial asset by about $10°C$.

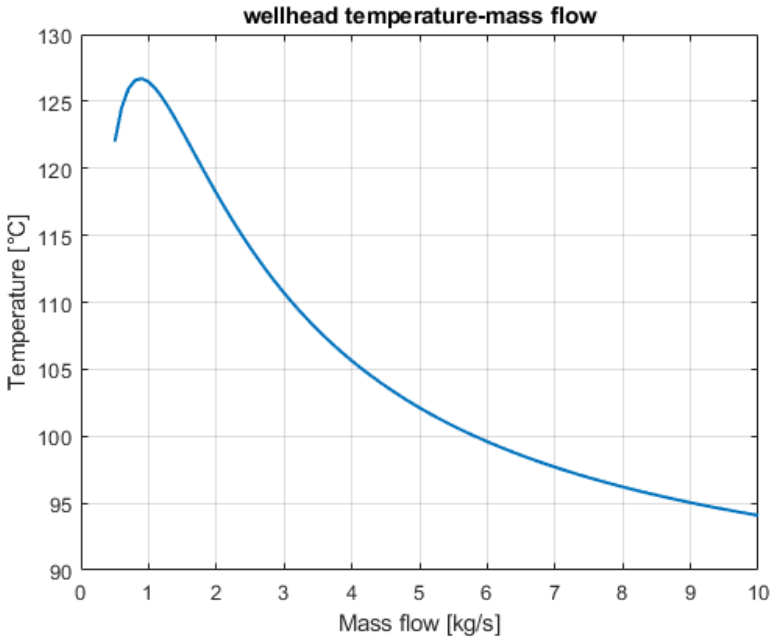

Figure 5.24: Wellhead coaxial temperature by varying Mass flow taking into account stratigraphy

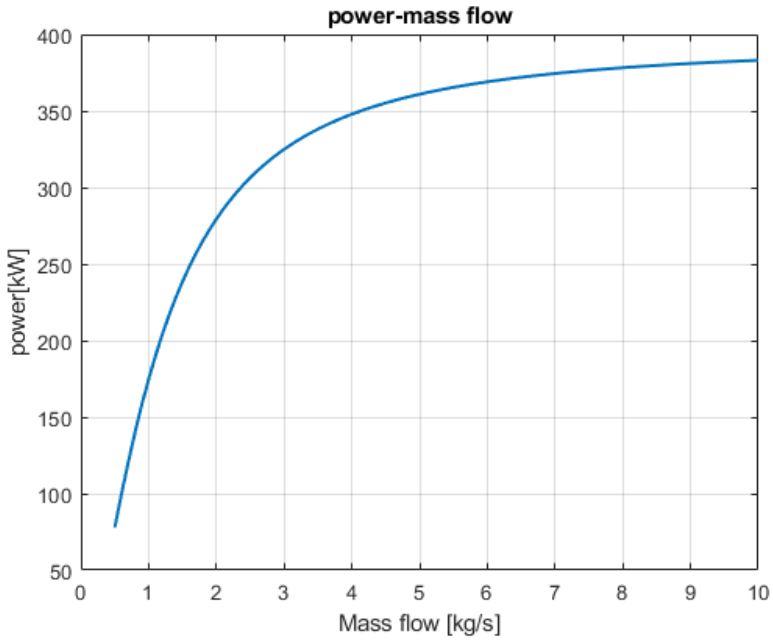

Figure 5.25: Power Coaxial temperature behavior when the mass flow rate changes taking into account stratigraphy

For all the values of mass flow the wellhead temperature and the power extracted are improved.

5.2.2 U-tube closed loop configuration

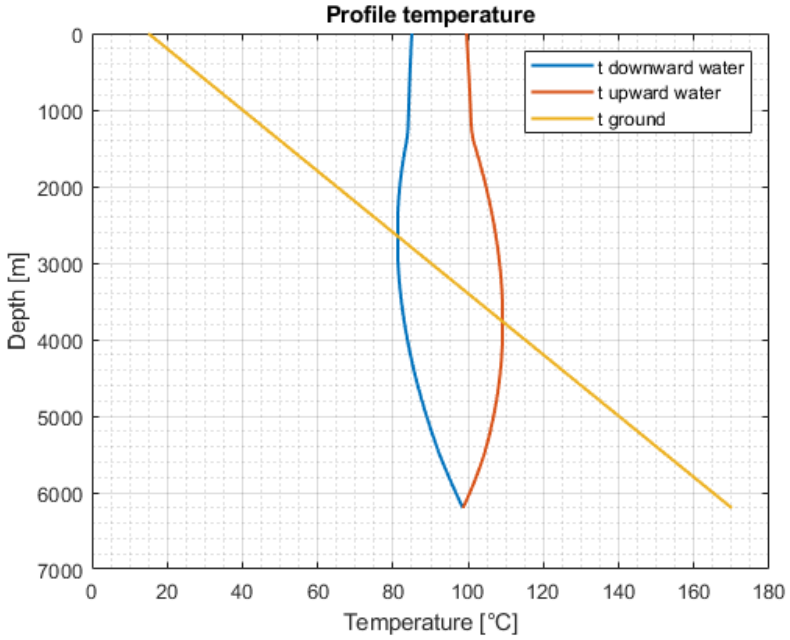

Figure 5.26: Profile temperature in the U-tube configuration taking into account stratigraphy

In the U-tube profile temperature the influence of the first thickness of ground is also very visible in the ascending fluid, indeed in this configuration both downward and upward tube is in contact with the ground.

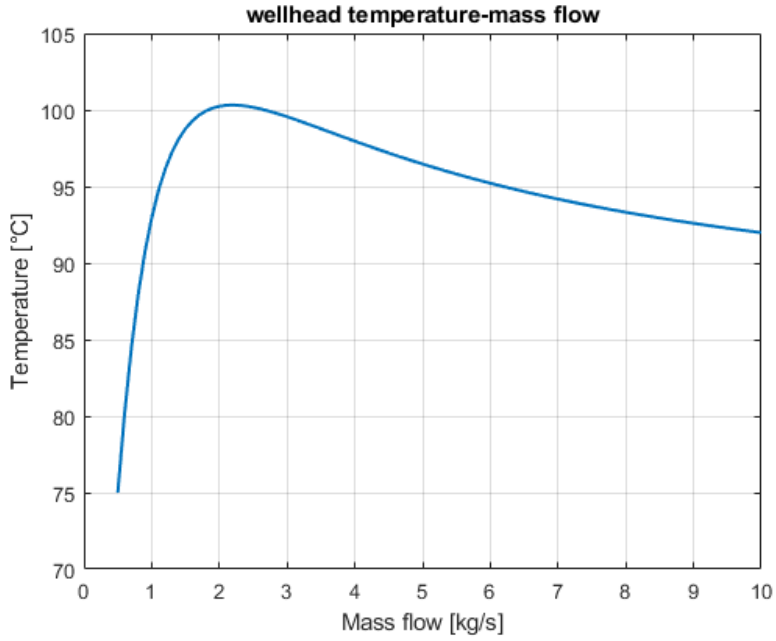

Figure 5.27: Wellhead U-tube temperature behavior when the mass flow rate changes taking into account stratigraphy

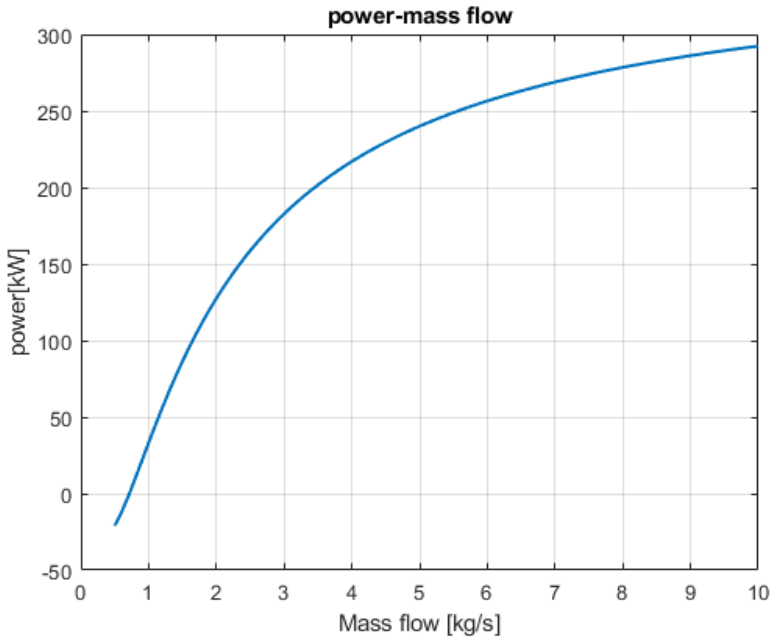

Figure 5.28: Power U-tube temperature behavior when the mass flow rate changes taking into account stratigraphy

5.2.3 Open loop configuration

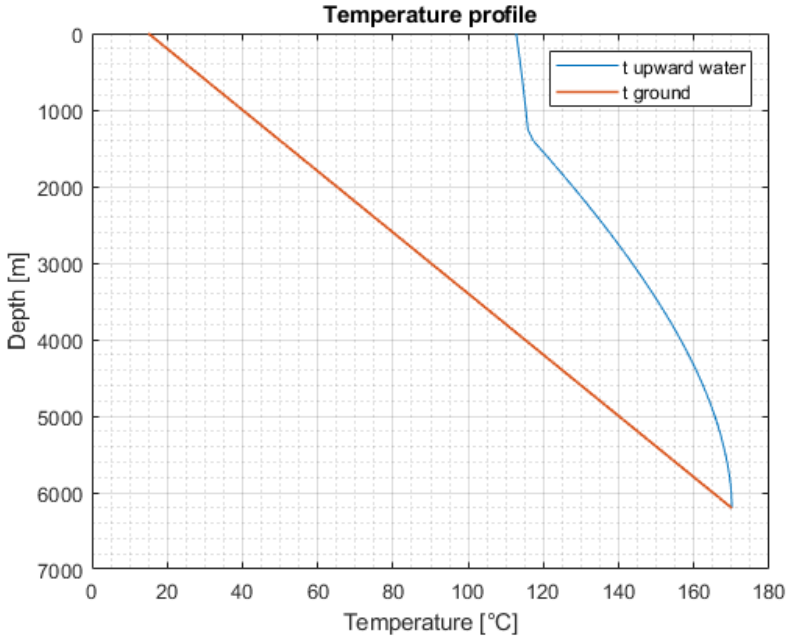

Figure 5.29: Profile temperature in open loop configuration taking into account stratigraphy

The exchange with the ground is increased ad so from 6202m to 1405m the heat losses are higher than the constant configuration.it's due largely by the conductivity of the rock because it is higher than the constant value. But in the last part from 1405m up to the surface the heat exchange is not good so an higher wellhead temperature occur.

Considering the ground properties dependent on depth the wellhead temperature increase of around $12°C$ compared to the same configuration with constant ground properties.

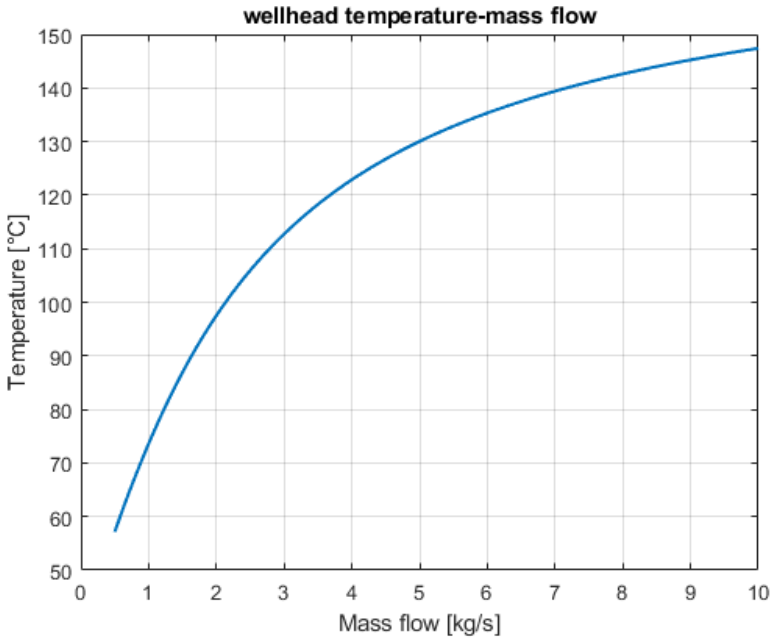

Figure 5.30: Wellhead open loop temperature by varying Mass flow taking into account stratigraphy

As can be seen in the fig 5.30 the wellhead has an improvement for all the values of mass flow. The benefits are more visible for low mass flow values. For a value of 0.5 $\frac{kg}{s}$ the temperature difference is around $20°C$, instead at a value of 10 $\frac{kg}{s}$ the temperature difference is less than $10°C$.

5.3 Coaxial heat exchanger optimization

In the last part of the work a computational intelligence-based approach was applied to the design of the coaxial heat exchanger.
The purpose of optimization is to understand the potential of this technology from an energy and economic point of view, this is done thanks to a multivariable optimization in which the search for the most appropriate configuration is made by varying all the parameters to be optimized simultaneously, thus ensuring the achievement of one of the best configurations for the objective function taken into consideration.
The design variables are the inner pipe, the insulating thickness, the mass flow and the input temperature.
One of the main variable influenced by the parameters to be optimized is the fluid velocity, it depends on two variables the flow rate and the passage area which is influenced by the radius of the inner tube and the thickness of the insulator, which takes away space from the annulus. Since the convective exchange prevails, if the velocity is too low the heat acquired in the downward pipe is lost in the upward. instead if the fluid has a high velocity the exchange in the downward tube is penalized, because there isn't enough time for the heat exchange so the wellhead temperature will be lower.
The velocity is also fundamental in the evaluation of the pressure loss, which depend on it quadratically.
The classical conventional optimization methods are iterative algorithms that exploit deterministic transition rules. The deterministic method if it runs on the same input, produces always the same output. The methods implies a starting or initial guess of the solution and iteratively refine the guess. For non-linear problem, most of the methods implies a linearization of the problem (by differentiation).
Deterministic local search methods have many pros as time-efficiently, stability and state of the art of the optimization techniques, but the worst disadvantage is that can be easily trapped in some of the local minima of an objective function without finding the global optimum solution.
Global search metaheuristics are time-consuming, due to its high computational cost, but can reach the global minimum whatever the objective function is.

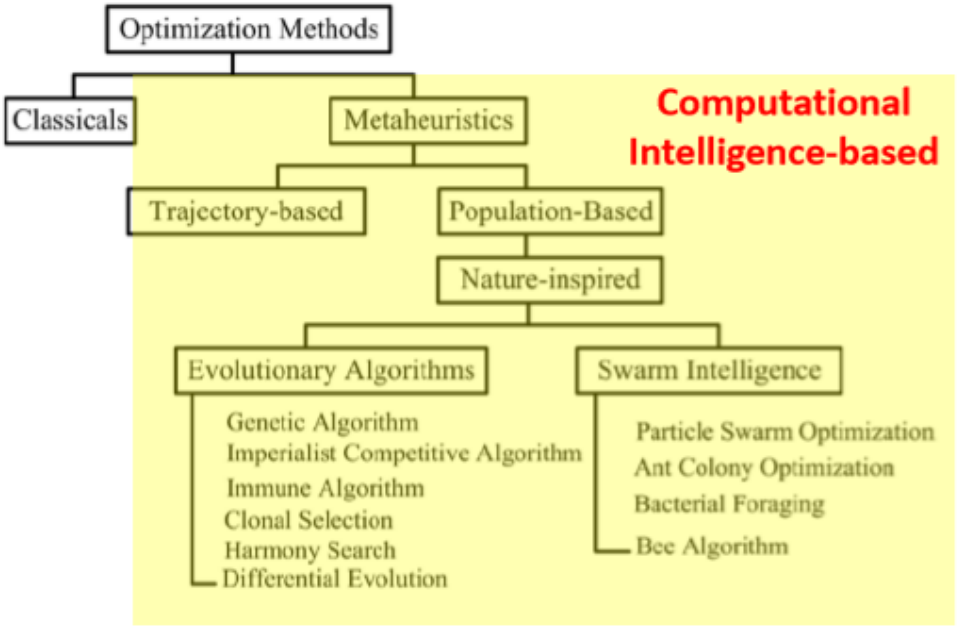

Figure 5.31: Optimization methods

The metaheuristic methods are iterative generation processes which are able to sampling and exploring an objective function landscape,thanks to the intelligent application of different concepts, and while the space is explored learning strategies are used to try to efficiently find the optimal solution. The reaching of the global minimum is helped by a use of stochastic transition rules.

Metaheuristic approaches have been well known for many years as an alternative to deterministic ones.

The need for stochastic approaches was born in the 1900s for the simulation and modeling of complex processes in various scientific fields.

In past years the biggest problem with this approach has been the high computational cost and the poor technological requirements in those years. Recently, thanks to the great increase in the computing power of devices, the metaheuristic approach is catching on in many sectors.

5.3.1 Swarm intelligence

The swarm intelligence is inspired by natural observations, on incredible abilities of a flock to overcame a daily problem. The individual,belonging to the swarm, don't need to have an explicit knowledge of the global structure.
A single individual is not able to evaluate a global situation, to centralize the information from the other individual and to direct others. A social colony is a decentralized system, the individuals belonging to the colony and they are distributed in the environment. The rules, that govern the movements of the individuals, are based only on local information from the individuals without the global environment information.
Computational intelligence paradigms population-based differ from traditional search in that:

- - Use a population of points (agents) in their search
  - Each point represents a solution to the problem
  - Large model space domain to search the solution
  - Number of solutions, generated and tested, orders of magnitude higher
  - The points(agents) interact each other with an intelligent behaviour;

- Use stochastic rather than deterministic transition rules (they are not pure probabilistic techniques because of the use of some strategy);

- Use direct "fitness" information, instead of function derivatives.

The particle swarm optimization is an heuristic optimization method proposed by Kennedy and Eberhart in 1995 [41] and is based on two main concept:

- Simulation of the swarm intelligence and the behavior of flock of birds and fish.

- Evolutionary computation. Due to its many advantages, including easy implementation, its level of coherence and coordination, the algorithm is widely adopted in several fields such as optimization process, model classification, machine study, neural network training.

The PSO works in a space M, with N dimensions, and the models are characterized by the following equations[42]:

$$l_q \leq x_{iq} \leq u_q \tag{5.1}$$

$$1 \leq q \leq n \tag{5.2}$$

$$1 \leq i \leq N \tag{5.3}$$

Where l_q and u_q are the upper and the lower bound of the parameters to be optimized (q) for each particle (i). Each particle, belonging to the swarm composed by N individual, is characterized by n-sized vector, each component of the vector represented a value of the design variable.
The swarm optimization starts with a randomly generated of particles in the specific space delimited by the boundaries, previously selected, and with a velocity equal to zero. Local and global bests are then calculated. the following steps, up to the limit generation value, are performed with the same procedure.
At each discrete time step (k^{th} iteration), each particle is located in the search space which fitness is evaluated by the objective function f(x). At each step (k) the particles position is updated by using a displacement vector called velocity, represented as[43]:

$$v_i^{k+1} = \omega^k \cdot v_i^k + \gamma_1 \cdot \alpha_1 \cdot (P_i^k - x_i^k) + \gamma_2 \cdot \alpha_2 \cdot (G^k - x_i^k) \tag{5.4}$$

Each particle (i), at the k^{th} iteration (from 0 to T, upper generation limit), samples the search space according to its own misfit history ($P_i(k)$) and to swarm experience G(k). So the velocity vector mixes a individual particle memory and the knowledge gained by the swarm.
ω, α_1 and α_2 are user supplied coefficients, instead γ_1 and γ_2 give the randomness components to the velocity.

- ω is the inertia weight ($0.8 \leq \omega \leq 1.2$ [44]), it is useful to keep the particle moving in the same direction it was originally heading. The speed convergence is helped by a lower value of this parameter, because it promote local exploitation.

- The second term (cognitive component) contain the cognitive attraction coefficient α_1 ($0 \leq \alpha_1 \leq 2$), this term attract the particle to its best solution, causing a draw back to the region of the search space already explored.

- The third term (social component) contain the social attraction coefficient α_2 ($0 \leq \alpha_2 \leq 2$). It causes the particle migration toward the best solution find by the swarm, high values favor faster convergence.

A stochastic behavior is given by the two random terms γ_1 and γ_2 which influenced the velocity vector and make the particle movements semi-random.

The stability of the PSO is guaranteed by the following inequalities [45]:

$$0 < \alpha_1 + \alpha_2 < 4 \tag{5.5}$$

$$\frac{\alpha_1 + \alpha_2}{2} - 1 < \omega < 1 \tag{5.6}$$

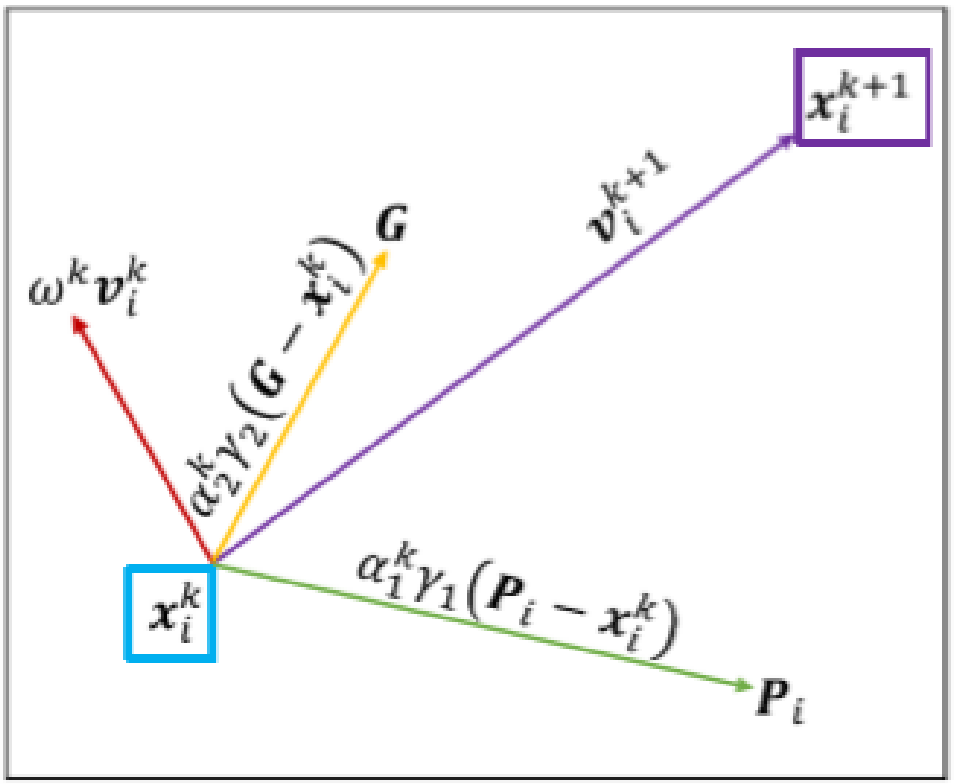

Figure 5.32: Velocity vector representation

For each particle x_i at each time step the position x_i^k is updated at x_i^{k+1} using the velocity vector v_i^{k+1}, the new position is evaluated as [43]:

$$x_i^{k+1} = x_i^k + v_i^{k+1} \tag{5.7}$$

To take into account the constraints and search the optimal result in the interested space three different methods are usually implemented: penalize, absorb, nearest.
The first method penalized the particles out of boundaries assigning them high values of the objective function. the particle is free to move across the constrains , they are attracted by the feasible area (with a lower value of the objective function) where they can return. In the absorb method

the boundaries can't be crossed by the particles and so the objective function can't be calculated out of the interested space. This method is useful to find the optimum value if it is very near to the bounds. The nearest method places the particles that violated the constrains on the nearest boundary, evaluating the fitness value.
In this work the penalized method is used.

5.3.2 Swarm optimization program check

Once the code for optimization with the application of swarm intelligence was readjusted for the problem of interest, its reliability was tested through the application of case studies whose results were already known. An example of this method was the calculation of the minimum pumping power, knowing that the power was minimized with a minimum flow rate and insulation thickness and maximum radius of the internal tube.
The ranges of the input parameters are:

- Insulating tube radius=0.05-0.07 [m];
- Inner tube radius=0.03-0.04 [m];
- Mass flow=3-7 [$\frac{kg}{s}$].

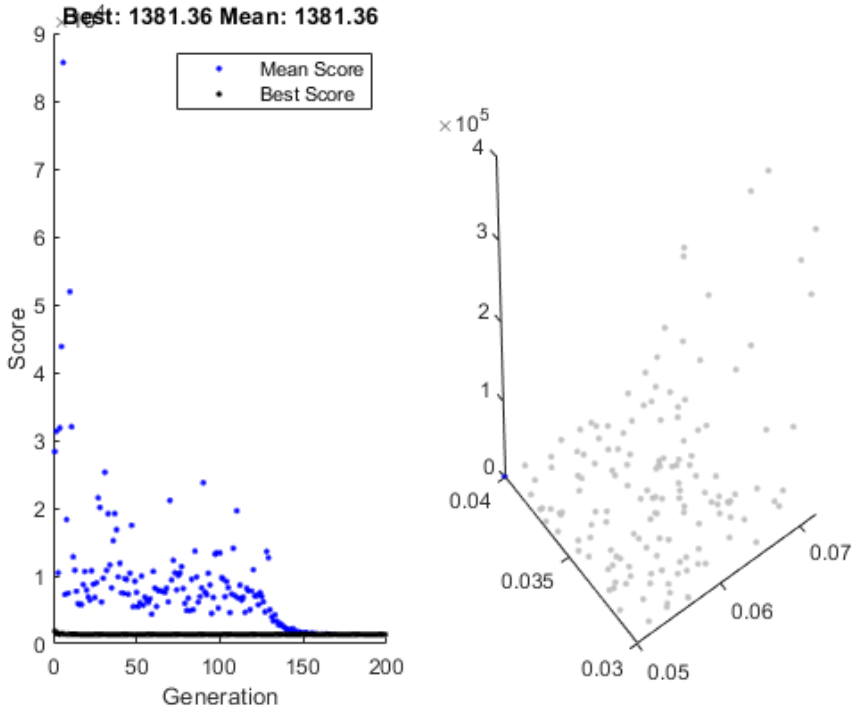

Figure 5.33: Swarm optimization result for minimum pressure loss

In the figure above 5.33 it can see the results of the two first parameters (insulating ad inner tube radius) which turn out to be respectively 0.05 and 0.04, as expected. The Mass flow, not shown in the graph, optimized from the point of view of pressure losses is 3 [$\frac{kg}{s}$], this too as expected.

5.3.3 Efficiency optimization with a fixed heat power

In the first type of optimization we tried to extract 300 kW heat power in the best way, so maximise the efficiency of the wellbore heat exchanger.
The PSO software works minimizing the objective function, so the function used is:

$$Ob_f = |Q_{th} - 300000| + 1500 \cdot \frac{1}{\eta_{wellbore}} \tag{5.8}$$

The first term ($|Q_{th} - 300000|$) measures the distance between the thermal power extracted from the considered configuration and the reference power of 300 kW. The closer the configuration is to 300 kW, the smaller this term will be making the objective function more optimal.
The second part ($1500 \cdot \frac{1}{\eta_{wellbore}}$) allows us to find the configuration with the greatest efficiency, If the efficiency is low, the term, including the inverse of the efficiency, acquires high values and therefore going to penalize the objective function with high values of it.
The coefficient that multiplies $\frac{1}{\eta_{wellbore}}$ helps to give importance to them in the function, increasing the orders of magnitude of the inverse of the efficiency.
The efficiency is defined as:

$$\eta_{wellbore} = \frac{Q_{th}}{W_{el}} \tag{5.9}$$

We have chosen 300 kW to give power to a small district heating power plant or to a factory in the nearby of the well.
The result of the optimization is shown in the figure below.

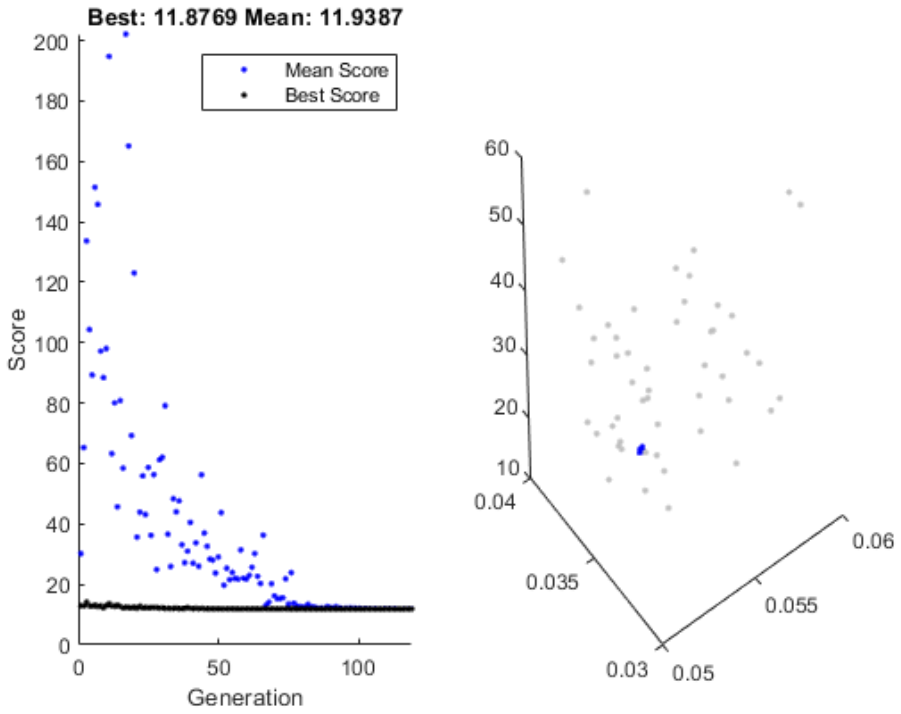

Figure 5.34: Swarm optimization result for a 300 kW heat power

The optimal configuration found is:

- Insulating tube radius=0.0544 [m];
- Inner tube radius=0.0378 [m];
- Mass flow=3.1515 [$\frac{kg}{s}$];
- Input fluid temperature=83$^{\circ}C$;

The heat power is 300 kW and the electric power, used for the fluid circulating, is 2,376 kW. The efficiency of the system with this configuration is 126,27 $\frac{kW_{th}}{kW_{el}}$, so with an expenditure of 1 electric kilowatt 126,27 heat kilowatt are extracted from the well.

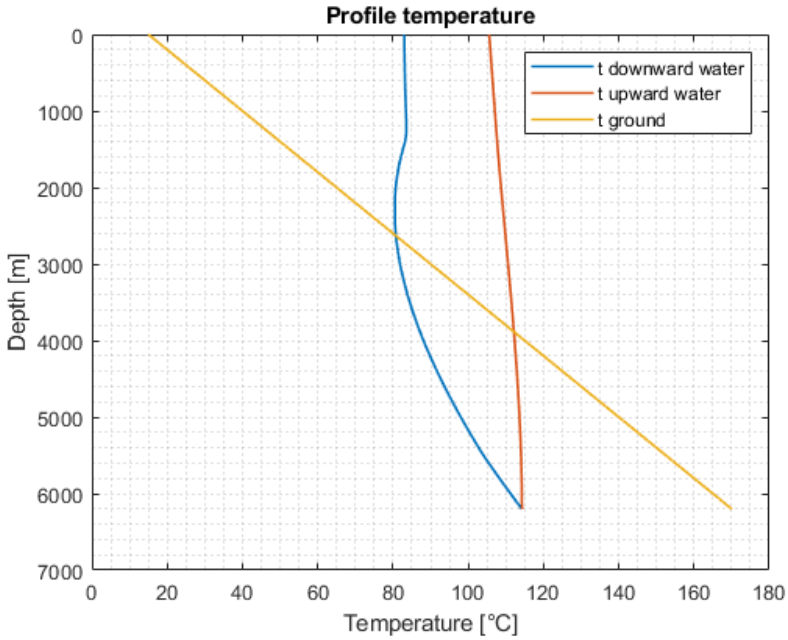

Figure 5.35: Optimized heat exchanger profile temperature

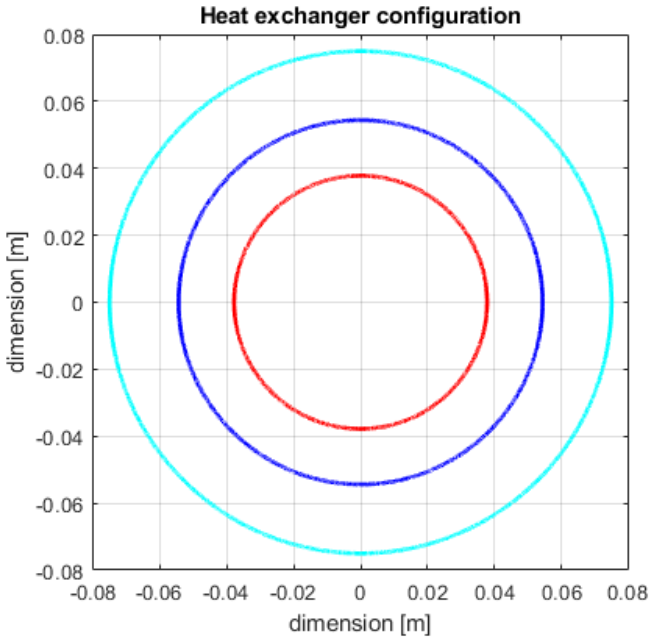

Figure 5.36: Optimized heat exchanger geometry

The value of the upward fluid heat losses is due mainly by two contribution. The inner tube radius is lower so the upward velocity is bigger therefore this decrease the residence time, and so also the heat losses improving the wellhead temperature. The second element is the thickness of the insulating material which has decreased compared to the previous configuration, and this parameter affect mainly the losses causing a greater loss of temperature of the rising fluid. This asset change is due to minimize the pumping power and so to maximize the efficiency.

5.3.4 Optimization to maximize gain

In the last optimization the focus isn't longer to performance but to an economic aspect. The optimization try to maximize the objective function that take in account the heat and the electric energy cost.
The objective function used is:

$$Ob_f = \frac{1}{G} + 10 \cdot (T_{wellhead} < 105) + 10 \cdot (\frac{1}{G} < 0) \tag{5.10}$$

The first term ($\frac{1}{G}$) taken into account the hourly gain. In fact, if the hourly gain increases the term that takes into account it is minimized.
The second part ($10 \cdot (T_{wellhead} < 105)$) ensures an outlet temperature of at least 105 Celsius degrees. When in a considered configuration a wellhead temperature lower than 105 is recorded the term ($T_{wellhead} < 105$) becomes equal to 1 and therefore a quote given by the multiplying factor that precedes it is added (in this case 10). The multiplier value must be large enough to correctly weight the term ($T_{wellhead} < 105$) in the objective function.
When, in a considered configuration, the costs exceed the earnings, the term G becomes negative (and so also $\frac{1}{G}$), since the PSO code searches for the minimum of the objective function, it would be taken into account as a solution. But being that we only want solutions where hourly revenues are positive the third term is inserted. In fact if a loss in a configuration taken into consideration is recorded (so ($\frac{1}{G} < 0$) becomes equal to 1) a value of 10 is added to the objective function excluding it from the optimal values, as in the case of a solution with a wellhead temperature lower than $105°C$.
The hourly earning is evaluated as:

$$G = Q_{th} \cdot C_{th} - W_{el} \cdot C_{el} \tag{5.11}$$

Where:

- C_{th} is the sell price of the heat energy [$\frac{euros}{kWh}$]

- C_{el} is the price of the electric energy [$\frac{euros}{kWh}$]

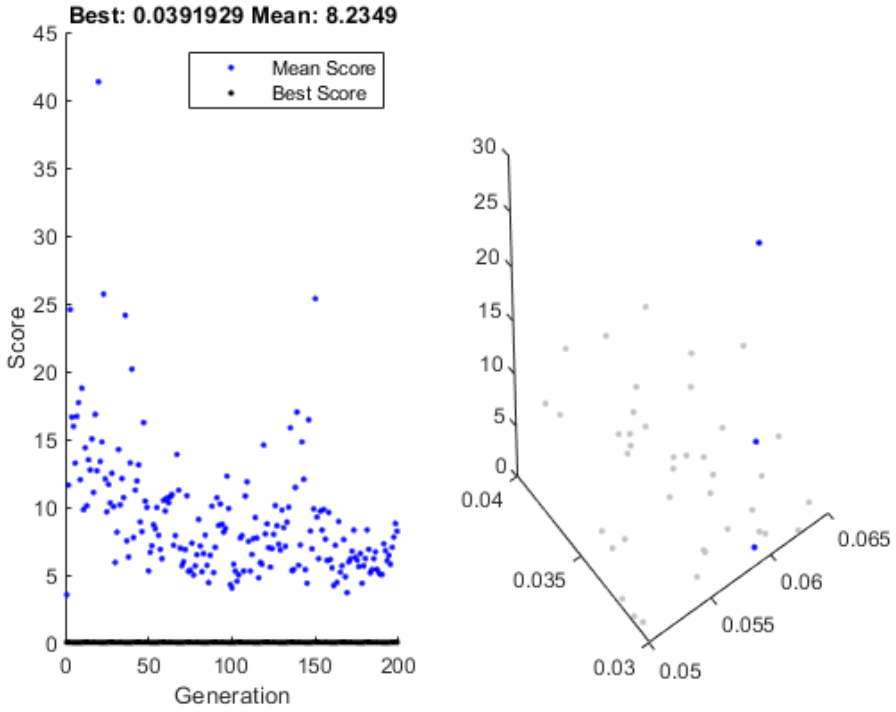

Figure 5.37: Swarm optimization results to obtain the maximum gain

The optimal configuration found is:

- Insulating tube radius=0.0594 [m];
- Inner tube radius=0.0305 [m];
- Mass flow=3.7786 [$\frac{kg}{s}$];
- Input fluid temperature=83$°C$;

The heat power extracted is 350,41 kW and the electric power absorbed is 11,38 kW. The hourly gain is 26,8 $\frac{euros}{h}$ and the efficiency is reduced at 30,79 $\frac{kW_{th}}{kW_{el}}$.

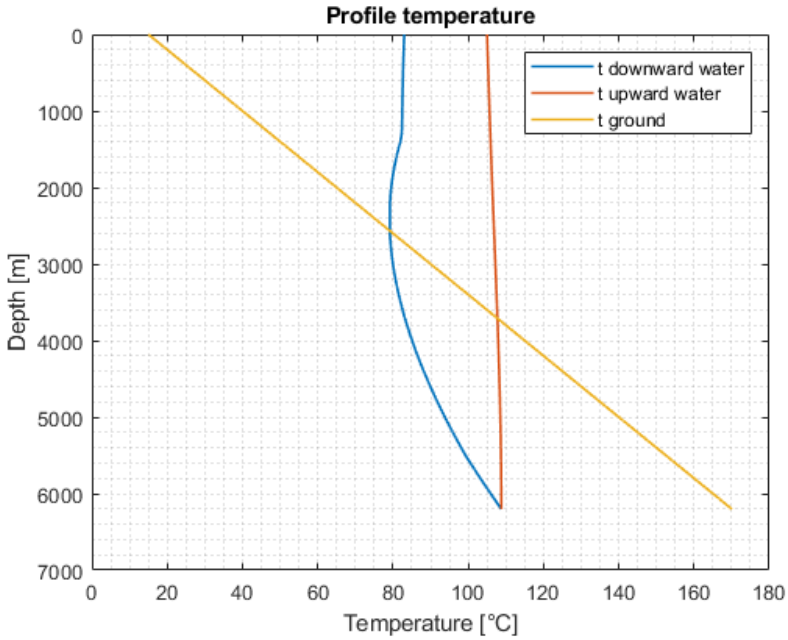

Figure 5.38: Optimized heat exchanger profile temperature for the maximum gain

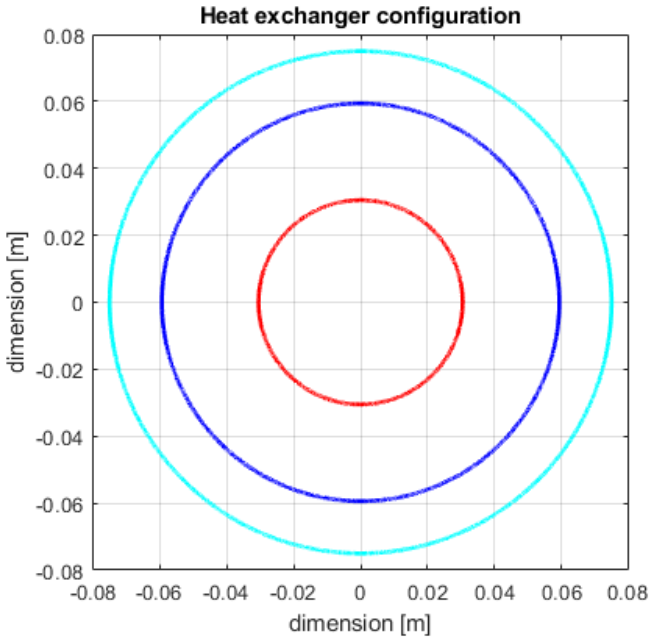

Figure 5.39: Optimized heat exchanger geometry for the maximum gain

6. Conclusions and future perspectives

In the early stages of the thesis work, two Matlab models were developed as reported in the results chapter (5). The outcomes obtained are the effect of the application of the two elaborated models, firstly considering the constant thermal and geological properties of the soil, secondly taking into consideration the specific properties of the site described in chapter 2 (Villafortuna-Trecate area). From the analysis of the graphic results obtained as output from the developed models (U-tube and Coaxial) it can see how, fixed the study case and its own parameters, a coaxial heat exchange configuration turns out to be more performing for each configuration considered. In details, from the comparison between the images 5.1 5.7 that report the temperature profile when the depth changes for the mass flow value fixed (3 $\frac{kg}{s}$), it can be noted that the outlet fluid temperature for the coaxial configuration (103°C) is higher than that estimated for the U-tube configuration (88°C). Also from the analysis of the curves shown in fig 5.3 5.8, it is possible to confirm, even when the flow rate varies, an ever higher output temperature of the coaxial configuration at the expense of the U-tube one.

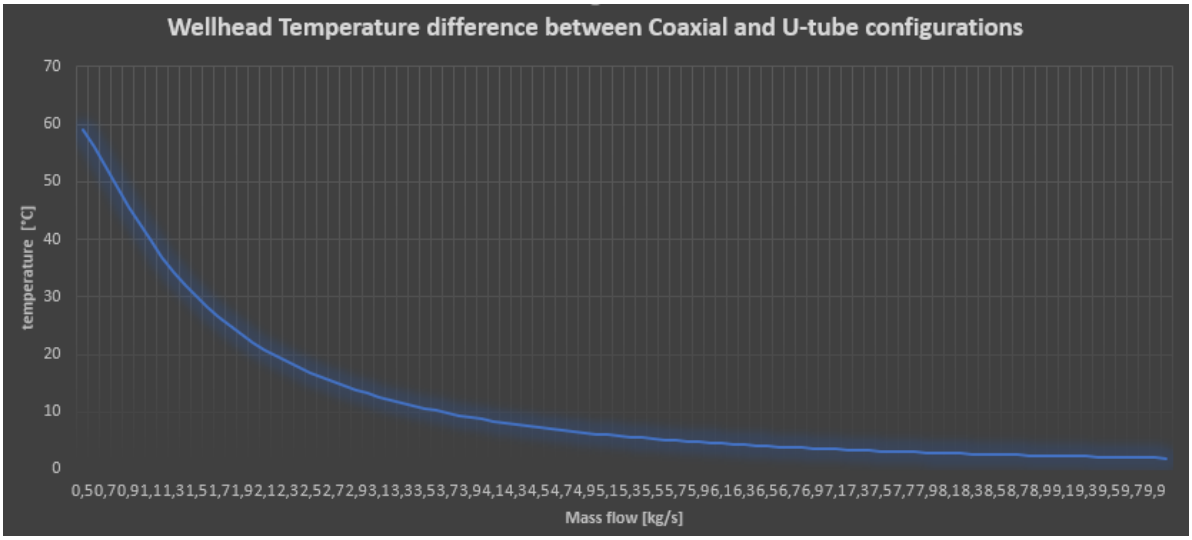

Figure 6.1: Difference between wellhead coaxial and u-tube temperatures

The thermal powers are consequently higher (comparison fig 5.4 and 5.9).
As regards the influence of stratigraphy and thus of the thermal and geological parameters related to it, from the comparison between figures 5.1 and 5.23 it is possible to elaborate the following considerations:

- The presence of a surface thickness of deposits characterized by low conductivity and specific heat values influences the heat exchange negatively, limiting the phenomenon of heat dispersion;

- The implementation of the correct stratigraphy in the model contributes to improving the heat exchange phenomenon at greater depths in correspondence with these thicknesses, the values of the thermal parameters are higher than those previously set (model without stratigraphy).

Given the considerations just reported, the application of the correct stratigraphic parameters within the models, which allow the reconstruction of the heat exchange mechanisms in such contexts, turns to be fundamental.

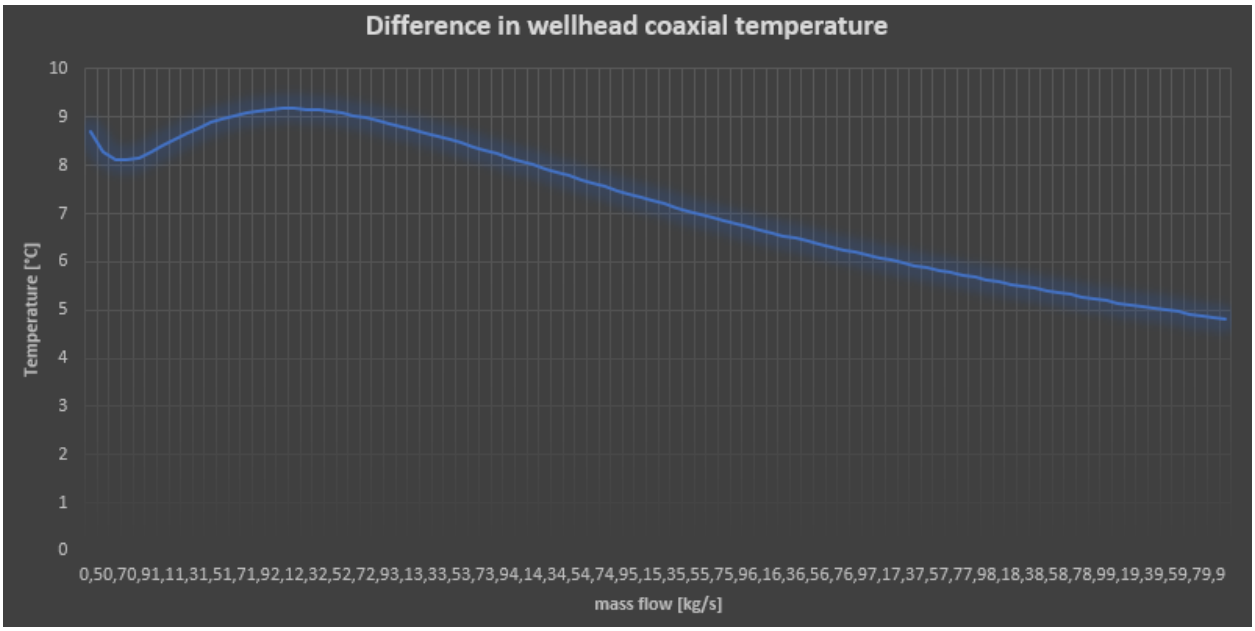

Figure 6.2: Difference between wellhead with and without stratigraphy temperatures

In addition to what has been said above and in order to understand how any changes in the parameters associated with the geological properties of the subsoil affect the thermal output values of the models, sensitivity analyzes were conducted.
By analyzing the results obtained, it is possible to underline how the parameter that most influences the thermal output values is the same that acts most on the thermal resistance value of the soil that is conductivity (figures 5.18 5.19).

After identifying the best performing closed loop configuration and understanding the importance of taking into consideration the stratigraphy of the site concerned, two different optimization processes was carried out.
In the first optimization process performed, the importance was given to the energy aspect and, above all, to the efficiency of the well.
A new geometry of the coaxial pipe was obtained, with a substantial reduction of the insulation pipe. This potential reduction can allow to contain the pressure drops and therefore also the pumping power, all this at the expense of the heat losses of the ascent tube and therefore creating a greater temperature difference between the head and the bottom of the well.
In order to try to limit this phenomenon, by increasing the thickness of insulation, the inner tube has been reduced, resulting in an increase in the pumping quota due to the ascent.
This geometry associated with a suitable flow rate allows to extract 300 thermal kW by spending 2,376 kW electric therefore obtaining an efficiency of 126,27 $\frac{kW_{th}}{kW_{el}}$.
By means of limiting electricity consumption rates, it is also possible to contain, if the origin of the electricity comes from the national energy mix and therefore also from thermo-electric plants, the consumption of hydrocarbons which are responsible for the production of substances that may be of local or global interest such as climate-altering gases.
The extraction of high efficiency thermal power allows to have a lesser impact on the environment and climate (one of the greatest challenges of these times) producing lesser quantities of greenhouse gases such as CO_2 and N_2O.
Secondly, an economic approach has been used for developing a second type of optimization process to understand the potential in terms of earnings of this technology coupled with a direct use of the extracted heat.
Also from this optimization the radius of the insulation pipe was less, even if not at the levels of the first optimization. In contrast, the inner pipe is reduced almost as much as possible. By reducing the inner pipe also reduces the losses of heat rising, thanks to the new thickness of the insulation purchased due to the new internal radius, ensuring better insulation. This leads to an increase in pressure losses due to a higher speed in the ascent tube.
With this configuration the system can have an hourly profit margin of 26,8 euros, efficiency is drastically reduced (30,79 $\frac{kW_{th}}{kW_{el}}$) but we have more convenience in selling more thermal energy even if it is produced in a much less efficient way.
The open-loop configuration remains, from a purely energetic point of view, the best method for extracting heat from disused oil and gas wells, both for the wellhead temperature and for the flow rate values.
However, the interest in closed loops remains high due to the technical problems of the open loop of corrosion, scaling and re-injected fluid combined with all legislative problems, which greatly limit the potential of this technology.

With the main future aim to improve the accuracy of the model, with a view to implementing the developed analysis work, the resistances associated with the thickness of the pipes and the concrete outside the larger pipe, which allows the fixing of the heat exchanger to the ground, should be taken into consideration.
Moreover, the important basic assumption related to the constancy of the properties of the water throughout the crossing of the WBHE, has been considered in the work performed. As in real situations the water properties usually change, due to the effect of temperature and pressure (which varies greatly due to the hydrostatic pressure due to the depth), in future works, it will be required to analyze the behavior of the fluid as its system changes.
In addition, a study concerning the material for the insulation between the ring and the inner tube would allow to select the most suitable type of material, both from the point of view of the actual technical feasibility (for example insufflation) and also from the economic one (given the large length of the exchanger, even if the radius involved are small, the volume of insulation could be considerable and so also the cost).
Another component of the system that is not taken into account is the heat exchanger, that represents an important technology, located between the WBHE and the district heating distribution circuit. Its cost will depend on the type of exchanger considered and the heat exchange area used to exchange the power extracted from the well. In detail, the exchange area will depend on the heat exchange coefficient due to the type of exchanger, the thermodynamic regime and the difference in average logarithmic temperatures. The average logarithmic dt is influenced by the type of district heating used and the regime of use of the WBHE on which the wellhead temperature depends.
Therefore, an optimal point of the functioning of the whole system could be found.
A research about the cost of laying the WBHE in the well should be also carried out. Subsequently, knowing this value, an economic analysis should be made to understand the economic feasibility effect, calculating indices such as the net present value (NPV) of the cash flows in the period considered system life and pay back time (PBT).
Furthermore, a legislative analysis of the regulatory regimes potentially activated for the purpose of the retrofitting disused hydrocarbon wells by means of closed-loop technologies should be made.

References

[1] Craig M Bethke, Wendy J Harrison, Craig Upson, and Stephen P Altaner. Supercomputer Analysis of Sedimentary Basins. *Science*, 239(4837):261–267, jun 1988.

[2] Ferdinando Franco Cazzini. The history of the upstream oil and gas industry in Italy. *Geological Society Special Publication*, 465(1):243–274, 2018.

[3] F. Bertello, R. Fantoni, and R. Franciosi. Overview of the Italy's petroleum systems and related oil and gas occurrences. *70th European Association of Geoscientists and Engineers Conference and Exhibition 2008: Leveraging Technology. Incorporating SPE EUROPEC 2008*, 1(June):74–78, 2008.

[4] Anna Cazzola, Roberto Fantoni, Roberto Franciosi, Valter Gatti, and Manlio Ghielmi. From thrust and fold belt to foreland basins: hydrocarbon exploration in Italy. *AAPG, International Conference 2011*, 10374(Mi):2–5, 2011.

[5] Roberto Fantoni, Roberto Galimberti, Paola Ronchi, and Paola Scotti. Po Plain Petroleum Systems : Insights from Southern Alps Outcrops (Northern Italy)*. *Search and Discovery Article*, 20120:7 pp., 2011.

[6] M Bello and R Fantoni. Deep oil plays in Po Valley: Deformation and hydrocarbon generation in a deformed foreland. *World Petroleum*, (April):1–5, 2002.

[7] D. Sui, E. Wiktorski, M. Røksland, and T. A. Basmoen. Review and investigations on geothermal energy extraction from abandoned petroleum wells. *Journal of Petroleum Exploration and Production Technology*, 9(2):1135–1147, 2019.

[8] C. Alimonti and E. Soldo. Study of geothermal power generation from a very deep oil well with a wellbore heat exchanger. *Renewable Energy*, 86:292–301, 2016.

[9] Cheng W.L. Nian, Y.L. Evaluation of geothermal heating from abandoned oil wells, 2018. Energy 142:592–607.

[10] Kabir C.S. Hasan, A.R. Heat transfer during two-phase flow in wellbores., 1991. Part I–formation temperature. Proceeding of SPE Annual Technical Conference and Exhibition.

[11] Nowak W. Stachel A.A. Kujawa, T. Analysis of the exploitation of existing deep production wells for acquiring geothermal energy, 2005. J. Eng. Phys. Thermophys 78:127–35.

[12] Nowak W. Stachel A.A. Kujawa, T. Utilization of existing deep geological wells for acquisitions of geothermal energy., 2006. Energy 31:650–664.

[13] I.A. Charnyi. Movement of the boundary of change in aggregate state with body cooling or heating, 1948. Izv. OTNAN SSSR, No. 2.

[14] I.A. Charnyi. Heating of a critical area of formation in pumping of hot water into a well., 1953. Neft. Khoz., No. 3.

[15] Gendler S.G. Dyad'kin, Yu.D. Heat and mass transfer processes in extraction of geothermal energy, 1985. Izd. LGI, Leningrad.

[16] Xianbiao Bu, Weibin Ma, and Huashan Li. Geothermal energy production utilizing abandoned oil and gas wells. *Renewable Energy*, 41:80–85, 2012.

[17] Ma W. Gong Y. Bu, X. Electricity generation from abandoned oil and gas wells., 2014. Energy Sources, Part A: Recovery, Utilization and Environmental Effects, 36:999-1006.

[18] Michaelides E.E. Davis, A.P. Geothermal power production from abandoned oil wells, 2009. Energy 34:866–872.

[19] W.Q. Tao. Numerical heat transfer, 2011. 2nd ed. Xi'an: Xi'an Jiao Tong University Press.

[20] Li T.T. Nian Y.L. Wang C.L. Cheng, W.L. Studies on geothermal power generation using abandoned oil wells., 2013. Energy 59.

[21] Li T.T. Nian Y.L. Xie K. Cheng, W.L. Evaluation of working fluids for geothermal power generation from abandoned oil wells., 2014. Appl. Energy 238.

[22] H.J. Jr. Ramey. Wellbore heat transmission, 1962. J. Pet. Technol. 14:427-435.

[23] Ghoreishi-Madiseh S. Hassani F. Al-Khawaja M. Templeton, J. Abandoned petroleum wells as sustainable sources of geothermal energy., 2014. Energy 70:366–373.

[24] T. L. A. S. F. P. D. P.Dewitt. Introduction to heat transfer, 2011. Jefferson City USA: John Wiley Sons, pp. 516-517,524-525.

[25] F. Ruiz-Calvo, M. De Rosa, J. Acuña, J. M. Corberán, and C. Montagud. Experimental validation of a short-term Borehole-to-Ground (B2G) dynamic model. *Applied Energy*, 140:210–223, 2015.

[26] Marcotte D. Pasquier P. Short-term simulation of ground heat exchanger with an improved trcm, 2012. Renew Energy 46:92–9.

[27] K. Y. B. J. G. W. X. Wang. A comprehensive review of geothermal energy extraction and utilization in oilfields, 2018. Journal of Petroleum Science and Engineering.

[28] Xiaolei Liu, Gioia Falcone, and Claudio Alimonti. A systematic study of harnessing low-temperature geothermal energy from oil and gas reservoirs. *Energy*, 142:346–355, 2018.

[29] Milliken M. Geothermal resources at naval petroleum reserve-3 (npr-3), 2007. In: Thirty-second work. Geotherm. Reserv. Eng., Stanford, California.

[30] PopovichN Poplar N Reinhardt T, Johnson LA. systems for electrical power from coproduced and low temperature geothermal resources, 2011. In: Thirty-second work. Geotherm. Reserv. Eng., Stanford, California.

[31] Xin S. Li K. Gong B., Liang H. Effect of water injection on reservoir temperature during power generation in oil fields, 2011. In: Thirty-second work. Geotherm. Reserv. Eng., Stanford, California.

[32] Xin S. Li K. Hu B., Liang H. Electrical power generation from low temperature co-produced geothermal resources at huabei oilfield., 2012. In: Thirty-second work. Geotherm. Reserv. Eng., Stanford, California.

[33] Moyes CP Patterson PD Mckenna JR, Blackwell D. Geothermal electric power supply possible from gulf coast, midcontinent oil field waters. 2005. 5:34-40.

[34] Teodoriu C Burrufet MA Limpasurat A, Falcone G. artificial geothermal energy potential of steam-flooded heavy oil reservoirs., 2010. Int J Oil Gas Coal Technol 4:31-46.

[35] Bennet K. Power generation potential from coproduced fluids in the los angeles basin., 2012. p. 1-97.

[36] Butler SJ Sanyal SK. Geothermal power capacity from petroleum wells- some case histories of assesment., 2010. World Geotherm Congr, p. 25-9.

[37] Petroleum and Gas engineering. http://petroleumandgasengineering.blogspot.com/2016/01/permeability 2016.

[38] John R. Fanchi. Enhanced recovery and coal gas modeling, 2018. Principles of Applied Reservoir Simulation (Fourth Edition).

[39] Lisa Gieg, Tom Jack, and Julia Foght. Biological souring and mitigation in oil reservoirs. *Applied microbiology and biotechnology*, 92:263–82, 08 2011.

[40] Basel I. Ismail. Orc-based geothermal power generation and co2-based egs for combined green power generation and co2 sequestration, 2013. New Developments in Renewable Energy.

[41] Eberhart R. Kennedy J. Particle swarm optimization, proc. ieee international, 1995. Conference on Neural Networks, IV, pp. 1942-1948.

[42] A. Godio and A. Santilano. On the optimization of electromagnetic geophysical data: Application of the PSO algorithm. *Journal of Applied Geophysics*, 148:163–174, 2018.

[43] Alessandro Santilano, Alberto Godio, and Adele Manzella. Particle swarm optimization for simultaneous analysis of magnetotelluric and time-domain electromagnetic data. *Geophysics*, 83(3):E151–E159, 2018.

[44] Eberhart R. Shi Y. A modified particle swarm optimizer. evolutionary computational proceedings, 1998. IEEE World Congress on Computational Intelligence, May 1998, Anchorage, AK.

[45] Guzzella L. Ebbesen S., Kiwitz P. A generic particle swarm optimization matlab function, 2012. American control conference Fairmont Queen Elizabeth, Montreal, Canada.